Superparamagnetic effects in the linear magnetic response of polydisperse ensembles of nanoparticles suspended in a fluid

I. S. Poperechny *

Institute of Continuous Media Mechanics, Russian Academy of Sciences, Ural Branch, Perm 614018, Russia and Perm State National Research University, Perm 614068, Russia

(Received 2 December 2023; accepted 8 March 2024; published 4 April 2024)

Within a kinetic theory, the linear magnetic response of uniaxial single-domain particles suspended in a fluid is analyzed. The main qualitatively different types of frequency dependence of the longitudinal dynamic magnetic susceptibility of such particles are described. It is shown that superparamagnetic (related to orientation thermal fluctuations of the magnetic moment inside a particle) peculiarities of the response of a particle to a probing magnetic field are not fully determined by the ratio of anisotropy energy to thermal energy when a stationary bias field is applied. For a case where the indicated ratio is much greater than one, a simple approximate expression for the dynamic magnetic susceptibility of a particle is proposed. The developed approach is extended to polydisperse suspensions of noninteracting uniaxial nanoparticles. It is shown that polydispersity does not vanish away specific superparamagnetic features in the dynamic magnetic response of such systems. Quantitative estimates of the corresponding effects are performed in different frequency ranges of the applied field. It is demonstrated that under certain restrictions on the disperse composition of a suspension, the internal diffusion of the magnetic moment can lead to a splitting of the absorption spectrum of the system. The significant role of the bias field is revealed. In particular, it can cause an additional absorption maximum provided the particle-size distribution meets the outlined condition. Also, it enables one to assess how important it is to take into account superparamagnetism of particles: the effect of the biasing is stronger for particles with smaller anisotropy and thereby more pronounced superparamagnetic properties. A qualitative agreement of some of the inferences with the experimental data is briefly discussed.

DOI: 10.1103/PhysRevE.109.044601

I. INTRODUCTION

Superparamagnetic nanoparticles have been studied for many years, beginning from the classic papers of Néel [1] and Bean [2]. However, they are still of a great interest, particularly, due to broad perspectives for use in medicine and biotechnology [3–6].

It is well known that magnetic response of nanoparticles strongly depends on a medium within they are dispersed, and for each type of a carrier specific theoretical base is required to interpret experimental results. To date, kinetic theory of remagnetization (both in stationary and/or alternating magnetic fields) of mechanically fixed superparamagnetic particles is elaborated rather well, especially for those cases where interparticle interactions can be neglected; see, for example, Refs. [7,8].

Meanwhile, a consistent theory of magnetic response of nanoparticles suspended in a fluid is still being formed. In general, kinetics of magnetization of such particles involves not only random walks of the magnetic moment inside a particle but also rotational Brownian motion of the particle body [9–13]. Because of that, the relaxation spectrum of a suspended particle is predicted to be more versatile than that of an immobilized one [14,15]. This results in additional features of magnetic response; for example, in the presence of a bias field, the absorption spectrum of a uniaxial particle suspended in a fluid could include up to three peaks in different frequency bands (for mechanically fixed particles, two at most) [15].

One-particle theories (such as presented in Refs. [9–15]) help to reveal and understand physical mechanisms of remagnetization of the particle in an external magnetic field. However, at present, their predictions can hardly be verified by direct measurements—a single particle generates too weak of a signal. Nowadays, the vast majority of experiments are performed with macroscopic samples (ferrofluids) containing a huge number of suspended particles. The important thing is that particles in such systems are not identical but dispersed in size—this is a common feature of existing synthesis methods. Meanwhile, dynamic magnetic properties of an individual particle could strongly depend on the ratio between magnetic energy proportional to the volume of that particle and thermal energy. Thus, it is doubtful whether the specific peculiarities of the magnetic response of a particle are inherent (at least to some extent) for an ensemble of particles or they are just vanished away by the polydispersity—even when interparticle interactions are left aside.

The purpose of this paper is to clarify the specified issue. It is organized as follows. Section II defines an ensemble to be considered and introduces relevant physical quantities. After that, in Sec. III possible types of the longitudinal linear magnetic response of a single particle are described and

*ipoperechny@gmail.com

systemized. Further, in Secs. IV and V, the obtained results are extended to polydisperse ensembles of noninteracting particles; special attention is paid to superparamagnetic effects that appear due to internal (with respect to particle body) diffusion of the magnetic moment of particles. Lastly, a relationship between theoretical predictions and experimental results is briefly discussed in the final part of Sec. V and then some conclusions are summed up in Sec. VI.

II. DYNAMIC MAGNETIC SUSCEPTIBILITY: THE BASIC EQUATIONS

A. An ensemble of noninteracting particles

Let us consider a model ensemble of N noninteracting single-domain uniaxial ferromagnetic nanoparticles suspended in a fluid. It is assumed that all particles are characterized by the same anisotropy constant K and saturation magnetization M_s but their diameters may be different. The magnetic moment of the whole system is a sum of magnetic moments of individual particles:

$$\boldsymbol{\mu} = \sum_{i=1}^{N} \boldsymbol{\mu}_i. \tag{1}$$

The direction of the magnetic moment $\boldsymbol{\mu}_i$—it is set by the unit vector $\boldsymbol{e}_i = \boldsymbol{\mu}_i/\mu_i$—changes even if the macroscopic conditions are fixed. First, vector $\boldsymbol{e}_i$ thermally deviates from the easy magnetization axis characterized by the unit vector $\boldsymbol{n}_i$. Second, vectors $\boldsymbol{e}_i$ and $\boldsymbol{n}_i$ turn randomly, in common with the particle body that undergoes rotational Brownian motion due to collisions with molecules of a surrounding fluid.

At these conditions, the magnetic state of the ensemble is described by the joint distribution function $P(t, \boldsymbol{e}_1, \boldsymbol{n}_1, \ldots, \boldsymbol{e}_N, \boldsymbol{n}_N)$ that depends on orientations of magnetic moments and anisotropy axes of all particles and obeys the normalization condition

$$\int P(t, \boldsymbol{e}_1, \boldsymbol{n}_1, \ldots, \boldsymbol{e}_N, \boldsymbol{n}_N)\, d\boldsymbol{e}_1 d\boldsymbol{n}_1 \ldots d\boldsymbol{e}_N d\boldsymbol{e}_N = 1. \tag{2}$$

Observable magnetic and orientation characteristics of the system can be found by averaging the corresponding quantity with the function P. In particular, the phase average of the magnetic moment at instant t is equal to

$$\begin{aligned}\langle \boldsymbol{\mu} \rangle &= \left\langle \sum_{i=1}^{N} \boldsymbol{\mu}_i \right\rangle \\ &= \sum_{i=1}^{N} \mu_i \int \boldsymbol{e}_i\, P(t, \boldsymbol{e}_1, \boldsymbol{n}_1, \ldots, \boldsymbol{e}_N, \boldsymbol{n}_N) \\ &\quad \times d\boldsymbol{e}_1 d\boldsymbol{n}_1 \ldots d\boldsymbol{e}_N d\boldsymbol{e}_N. \end{aligned} \tag{3}$$

For noninteracting particles, the function P is reduced to a product of normalized distribution functions $W_i(t, \boldsymbol{e}, \boldsymbol{n})$ of orientations of magnetic moment and anisotropy axis of individual particles:

$$P(t, \boldsymbol{e}_1, \boldsymbol{n}_1, \ldots, \boldsymbol{e}_N, \boldsymbol{n}_N) = \prod_{i=1}^{N} W_i(t, \boldsymbol{e}, \boldsymbol{n}),$$

$$\int W_i(t, \boldsymbol{e}, \boldsymbol{n})\, d\boldsymbol{e}\, d\boldsymbol{n} = 1, \tag{4}$$

so

$$\langle \boldsymbol{\mu} \rangle = \sum_{i=1}^{N} \mu_i \int \boldsymbol{e}\, W_i(t, \boldsymbol{e}, \boldsymbol{n})\, d\boldsymbol{e}\, d\boldsymbol{n}. \tag{5}$$

Due to a huge number of particles in real systems, Eq. (5) is not suitable for a practical usage. If, to assume for simplicity that all particles are made of the same material, have the same thickness of surfactant layer, and the initial state of the system is not important, then there is the only distinguishing property of a particle—the diameter of its magnetic phase (magnetic core). Then, denoting the latter by d, let us introduce the microscopic density of number of particles as

$$\rho_s(d) = \frac{1}{N} \sum_{i=1}^{N} \delta(d - d_i), \quad \int_0^\infty \rho_s(d)\, dd = 1. \tag{6}$$

This quantity allows us to write an integral expression for the total magnetic moment of the system:

$$\langle \boldsymbol{\mu} \rangle = N \int_0^\infty \langle \boldsymbol{\mu}(d) \rangle\, \rho_s(d)\, dd; \tag{7}$$

here

$$\langle \boldsymbol{\mu}(d) \rangle = \mu(d) \int \boldsymbol{e}\, W(t, \boldsymbol{e}, \boldsymbol{n}; d)\, d\boldsymbol{e}\, d\boldsymbol{n} \tag{8}$$

is the average magnetic moment of the particle with magnetic diameter d (it is emphasized by the respective parameter of the function W).

Based on function $\rho_s(d)$, one can introduce a smoothed density function:

$$\rho(d) = \frac{\int_d^{d+\Delta d} \rho_s(y)\, dy}{\Delta d}, \quad \int_0^\infty \rho(d)\, dd = 1. \tag{9}$$

By means of the specified function, the magnetic moment of the system can be found as

$$\langle \boldsymbol{\mu} \rangle = N \sum_{n=0}^{\infty} \langle \boldsymbol{\mu}(n\,\Delta d) \rangle \rho(n\,\Delta d) \Delta d. \tag{10}$$

Usually, however, it is assumed that $\Delta d \to 0$ and the sum is replaced by an integral:

$$\langle \boldsymbol{\mu} \rangle = N \int_0^\infty \langle \boldsymbol{\mu}(d) \rangle\, \rho(d)\, dd. \tag{11}$$

In reality, the scale of coarsening Δd is determined by the capabilities of equipment used to analyze polydispersity.

B. Kinetic equation

In the absence of interparticle interactions, the orientation distribution function $W(t, \boldsymbol{e}, \boldsymbol{n}; d)$ in Eq. (8) obeys a closed evolution equation

$$\frac{\partial W}{\partial t} = \hat{S} W, \tag{12}$$

where $\hat{S}$ is the operator that determines orientation kinetics of the particle magnetization vector (kinetic operator).

In Refs. [9,16], it is shown that in the gyration-free approximation

$$\hat{S}W = \frac{1}{2\tau_B}(\hat{\boldsymbol{J}}_e + \hat{\boldsymbol{J}}_n)\cdot W(\hat{\boldsymbol{J}}_e + \hat{\boldsymbol{J}}_n)\left(\frac{U}{k_BT} + \ln W\right) + \frac{1}{2\tau_D}\hat{\boldsymbol{J}}_e \cdot W\hat{\boldsymbol{J}}_e\left(\frac{U}{k_BT} + \ln W\right), \tag{13}$$

where U is the orientation-dependent part of magnetic energy of the particle, T is the temperature of the system in absolute units, k_B is the Boltzmann constant, and vector operators $\hat{\boldsymbol{J}}_e$ and $\hat{\boldsymbol{J}}_n$ are defined according to

$$\hat{\boldsymbol{J}}_e = \boldsymbol{e}\times\frac{\partial}{\partial \boldsymbol{e}}, \quad \hat{\boldsymbol{J}}_n = \boldsymbol{n}\times\frac{\partial}{\partial \boldsymbol{n}}. \tag{14}$$

As it should, a Boltzmann function

$$W_0 = \frac{1}{Z}\exp(-U/k_BT), \quad Z = \int d\boldsymbol{n}\int d\boldsymbol{e}\,\exp(-U/k_BT) \tag{15}$$

is a solution of the equilibrium problem $\hat{S}W_0 = 0$. The times τ_B and τ_D in (13) are defined as follows:

$$\tau_B = 3\eta V_p/k_BT, \qquad \tau_D = (1+\alpha^2)\mu/2\alpha\gamma k_BT, \tag{16}$$

where η is dynamic viscosity of a fluid, V_p is hydrodynamic volume of the particle (for given values of d and d_s), α is the precession damping parameter, and γ is the gyromagnetic ratio. Time τ_B determines a rate of the rotational Brownian diffusion of the particle body and τ_D sets a timescale of internal (with respect to $\boldsymbol{n}$) superparamagnetic relaxation of the magnetic moment in a situation when thermal energy is much greater than the anisotropy one.

In the presence of the external magnetic field $\boldsymbol{H}$, the energy U is a sum of Zeeman and anisotropy terms:

$$U = -\boldsymbol{\mu}\cdot\boldsymbol{H} - KV(\boldsymbol{e}\cdot\boldsymbol{n})^2, \tag{17}$$

where V is volume of the magnetic core of the particle. In units of thermal energy function, (17) takes the form

$$\frac{U}{k_BT} = -\xi(\boldsymbol{e}\cdot\boldsymbol{f}) - \sigma(\boldsymbol{e}\cdot\boldsymbol{n})^2, \tag{18}$$

where dimensionless characteristics for magnitude of the magnetic field and the anisotropy energy are introduced:

$$\xi = \frac{\mu H}{k_BT}, \qquad \sigma = \frac{KV}{k_BT}. \tag{19}$$

C. Response function

Let us consider the case when the coaligned dc bias field $\boldsymbol{H}_0$ and linearly polarized ac field $\boldsymbol{h}(t)$ are applied to the system. In dimensionless units the overall field acting on the particle is equal to $\xi_0 + \xi(t)$, where $\xi_0 = \mu H_0/k_BT$ and $\xi(t) = \mu h(t)/k_BT$. It is assumed that amplitude of the ac field is relatively small, so that $|\xi(t)| \ll 1$. Then it is convenient to represent the kinetic operator $\hat{S}$ in the form

$$\hat{S} = \hat{S}_0 + \xi(t)\hat{S}_1, \quad \hat{S}_0 = \hat{S}(\xi_0) \tag{20}$$

and write the orientation distribution function as a sum of the equilibrium and nonequilibrium parts:

$$W = W_0 + W_t, \quad \hat{S}_0W_0 = 0. \tag{21}$$

In the linear approximation in $\xi(t)$, the function W_t obeys the equation

$$\frac{\partial W_t}{\partial t} = \hat{S}_0W_t + (\hat{S}_1W_0)\xi(t). \tag{22}$$

Its Fourier transform gives

$$(i\omega\hat{I} - \hat{S}_0)W^\omega = (\hat{S}_1W_0)\xi^\omega; \tag{23}$$

here $\hat{I}$ is the unit operator and ξ^ω and W^ω are Fourier images of the perturbation $\xi(t)$ and response W_t, respectively. Thus, in the frequency representation, the nonequilibrium component of the distribution function can be calculated as

$$W^\omega = [(i\omega\hat{I} - \hat{S}_0)^{-1}\hat{S}_1W_0]\,\xi^\omega. \tag{24}$$

Accordingly, the Fourier image of the average projection of the unit magnetization vector $\boldsymbol{e}$ (its variable component) onto the field direction is equal to

$$\langle\boldsymbol{e}\cdot\boldsymbol{f}\rangle^\omega = R(\omega)\,\xi^\omega, \tag{25}$$

where

$$R(\omega) = \int(\boldsymbol{e}\cdot\boldsymbol{f})[(i\omega\hat{I} - \hat{S}_0)^{-1}\hat{S}_1W_0]\,d\boldsymbol{e}\,d\boldsymbol{n}. \tag{26}$$

The function $R(\omega)$ completely determines the response of an isolated particle to a probing magnetic field. Below it is found numerically according to the method proposed in Ref. [16] and successfully used in Refs. [14,15]. In this approach, the kinetic operator and the function W_0 are set in the representation where the basis is built up by the so-called bipolar harmonics. With such a choice, the matrix of the kinetic operator comes out to be quite sparse and close to diagonal which simplifies calculations. The type of $R(\omega)$ significantly depends on values of the parameters σ and ξ_0 as well as on reference diffusion times τ_D and τ_B [it seen from Eqs. (13) and (18)].

D. Dynamic magnetic susceptibility of an ensemble

As a rule, in experiments with magnetic suspensions, the average projection M of the magnetization onto the unit vector $\boldsymbol{f} = \boldsymbol{H}/H$ along the applied field is measured. If particles are dispersed in the volume $V_{\rm sys}$ and their average concentration is $c = N/V_{\rm sys}$, then

$$M = \frac{\langle\boldsymbol{\mu}\rangle\cdot\boldsymbol{f}}{V_{\rm sys}} = c\int_0^\infty \mu(d)\,\rho(d)\,\langle\boldsymbol{e}\cdot\boldsymbol{f}\rangle\,dd,$$
$$\langle\boldsymbol{e}\cdot\boldsymbol{f}\rangle = \int(\boldsymbol{e}\cdot\boldsymbol{f})\,W(t,\boldsymbol{e},\boldsymbol{n};d)\,d\boldsymbol{e}\,d\boldsymbol{n}. \tag{27}$$

From Eqs. (25) and (27), it follows that the Fourier transform of the variable part of the magnetization is

$$M^\omega = c\int_0^\infty \mu(d)\,\rho(d)\,\langle\boldsymbol{e}\cdot\boldsymbol{f}\rangle^\omega dd = c\int_0^\infty \mu(d)\,\rho(d)\,R(\omega;d)\,\xi^\omega(d)\,dd, \tag{28}$$

with $\xi^\omega(d) = \mu(d)\,h^\omega/k_BT$; please note that the dependence of the response function on a particle size is indicated here explicitly via the parameter d (it seems expedient when discussing a polydisperse system).

Assuming for simplicity that every particle has a spherical shape, it is reasonable to introduce the dimensionless magnetic diameter $x = d/d_M$ with $d_M = (6k_BT/\pi M_s^2)^{1/3}$ as the length scale (use of the Gaussian unit system is supposed). Then,

$$M^\omega = \left(\frac{c}{k_BT}\int_0^\infty \mu^2(d)\,\rho(d)\,R(\omega;d)\,dd\right)h^\omega = \left(\frac{c\,k_BT}{M_s^2}\int_0^\infty x^6\,\rho(x)\,R(\omega;x)\,dx\right)h^\omega = \frac{c\,k_BT}{M_s^2}\,\tilde\chi(\omega)\,h^\omega. \tag{29}$$

The function

$$\tilde\chi(\omega) = \int_0^\infty x^6\,\rho(x)\,R(\omega;x)\,dx \tag{30}$$

is a theoretical analog of the dynamic magnetic susceptibility of the considered suspension; at given temperature, it completely determines linear response of the system to a probing magnetic field.

As mentioned above, magnetodynamic properties of a single particle depend on values of the parameters σ, ξ, τ_D, and τ_B. For a polydisperse system, these parameters, however, are not appropriate because they are all proportional to a particle volume. Instead, it is convenient to specify an ensemble by the following dimensionless quantities:

$$\kappa = \frac{K}{M_s^2},\quad q = \frac{H}{M_s},\quad x_s = \frac{d_s}{d_M},\quad \zeta_0 = \frac{(1+\alpha^2)M_s}{6\alpha\gamma\eta},\quad \rho(x)\quad \left(\int_0^\infty \rho(x)\,dx = 1\right), \tag{31}$$

which are correspondingly the anisotropy parameter, magnitude of the applied field, double thickness of the surfactant shell, viscosity parameter and the particle-size distribution function. As a timescale, it is suitable to use the reference time

$$\tau_M = \frac{1+\alpha^2}{2\alpha\gamma M_s} \tag{32}$$

that does not depend on particle size. With such a choice, the following relations hold: $\sigma = \kappa x^3$, $\xi = qx^3$, $\tau_D = \tau_M x^3$ and $\tau_B = \tau_M(x+x_s)^3/\zeta_0$.

Let us make estimates. With saturation magnetization $M_s \approx 400\,\mathrm{emu/cm^3}$ (typical value for ferrites), the diameter $d_M \approx 7-8$ nm in a wide temperature range. Double size of the surfactant shell is typically $d_s \approx 4$ nm, so $x_s \approx 0.5$. Parameter ζ_0 is expected to be in the range from $\sim 10^{-2} - 10^{-3}$ (for water) to $\sim 10^{-6}$ (for glycerin). Time τ_M is of order $10^{-10} - 10^{-7}$ s for typical ferrites with the precession damping constant $\alpha \sim 0.01 - 0.1$. Formally, the upper limit of integration in Eq. (30) is infinite but, in real samples, certainly, particles have finite diameters; for single-domain particles, $x \lesssim 5$.

Note, when the International System of Units is used, the definitions should be changed: $d_M = (24k_BT/\mu_0 M_s^2)^{1/3}$, $q = 4\pi H/M_s$, and $\kappa = 4\pi K/\mu_0 M_s^2$, where $\mu_0 = 4\pi \times 10^{-7}$ H/m.

III. RESPONSE FUNCTION OF A PARTICLE

A. Possible types

To characterize the linear magnetic response of an individual particle (or a monodisperse ensemble of particles), it is enough to get frequency dependencies of the real R' and imaginary R'' parts of the function R. Often, the so-called Cole-Cole diagrams, where the real part R' is read on the horizontal axis and the imaginary one R''on the vertical one, are also used.

All qualitatively different types of R can be found if one fixes the anisotropy parameter and varies both the particle size and magnitude of the bias field. Results are summarized in Figs. 1 and 2 where, for different magnetizing fields $q_0 = H_0/M_s$, the frequency dependencies $R''(\omega)$ and the corresponding Cole-Cole diagrams are shown for particles with diameters $x = 1$, 1.5, and 2.5; the curves are obtained for the anisotropy parameter $\kappa = 2$ and the viscosity parameter $\zeta_0 = 10^{-3}$. Thus, the following cases are possible:

(1) In the zero bias field, the function $R''(\omega)$ has a single peak in the frequency range $\omega\tau_M \sim 1$ and the corresponding Cole-Cole diagram is a semicircle passing through the origin [solid lines in Figs. 1(a) and 2(a)]. In the magnetizing field, an additional maximum can appear at frequency $\omega\tau_M \sim 1/\zeta_0$ [dashes and dots in Fig. 1(a)]. The respective Cole-Cole diagrams in Fig. 2(a) have a peculiarity on the right (low-frequency) edge. A response function of this type is typical for particles with the ratio of anisotropy energy to thermal energy $\sigma \lesssim 2.5$.

(2) In the zero bias field, the line $R''(\omega)$ has two peaks: one at frequency $\omega\tau_M \sim 1$, and the other – at a value smaller by about one or several orders [solid line in Fig. 1(b)]; when the bias field is applied, the additional—third—low-frequency maximum appears [see dashes and dots in Fig. 1(b)]. The corresponding Cole-Cole diagrams are like several connected arcs; see Fig. 2(b). A response function of this type is inherent to particles with $2.5 \lesssim \sigma \lesssim \sigma_*$; the upper limit σ_* decreases predominantly logarithmically when the ratio $\tau_D/\tau_B = \zeta_0\,(x/(x+x_s))^3$ raises (see Fig. 7 in Ref. [15]) and is expected to be in the range from $\sigma_* \approx 5$ to $\sigma_* \approx 17$. For example, $\sigma_* \approx 10$ at $\zeta_0 = 10^{-3}$ for particles of size $x = 1$ and the surfactant shell thickness $x_s = 0.5$.

(3) In the zero bias field, the spectrum $R''(\omega)$ has two maxima (low- and high-frequency), the magnetizing field changes their position and height, but does not lead to additional peaks [Fig. 1(c)]; the respective Cole-Cole diagram is shown in Fig. 2(c). A response function of this type is inherent to particles with $\sigma \gtrsim \sigma_*$.

The mechanisms of magnetic relaxation of a superparamagnetic nanoparticle suspended in a fluid and corresponding peculiarities of $R'(\omega)$ and $R''(\omega)$ are discussed in more detail in Ref. [15]. The high-frequency peak at $\omega\tau_M \sim 1$ (visible on all curves in Fig. 1) is associated with the so-called intrawell relaxation of particle magnetic moment near minima of the potential Eq. (18). With an increase in the ratio of anisotropy energy to thermal energy, the height of this peak diminishes and becomes zero at $\sigma \to \infty$. It should be noted that gyroscopic effects are not considered here (the gyration-free approximation is adopted), and the specified maximum is not related to ferromagnetic resonance. The low-frequency (in the

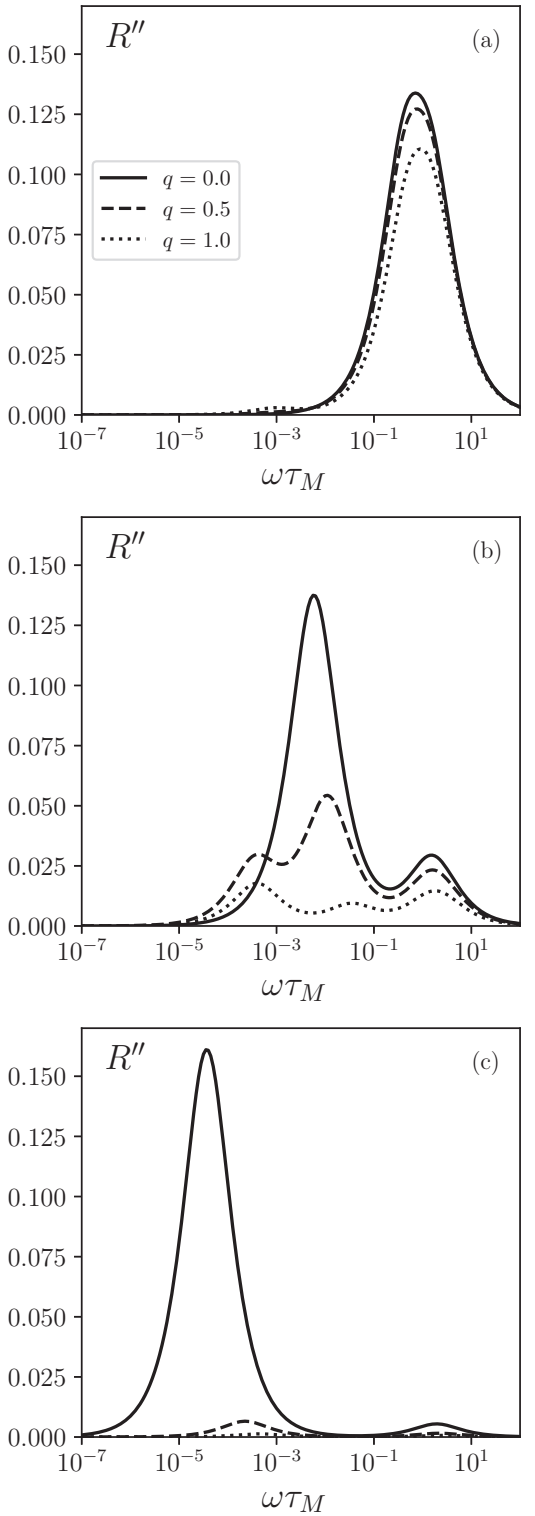

FIG. 1. Frequency dependencies of the imaginary part of the response function for a particle with size $x = 1$ (a), 1.5 (b), and 2.5 (c); solid lines: bias field $q_0 = 0$, dashes: $q_0 = 0.5$, dots $q_0 = 1$. Anisotropy parameter $\kappa = 2$, inverse viscosity $\zeta_0 = 10^{-3}$, surfactant thickness $x_s = 0.5$.

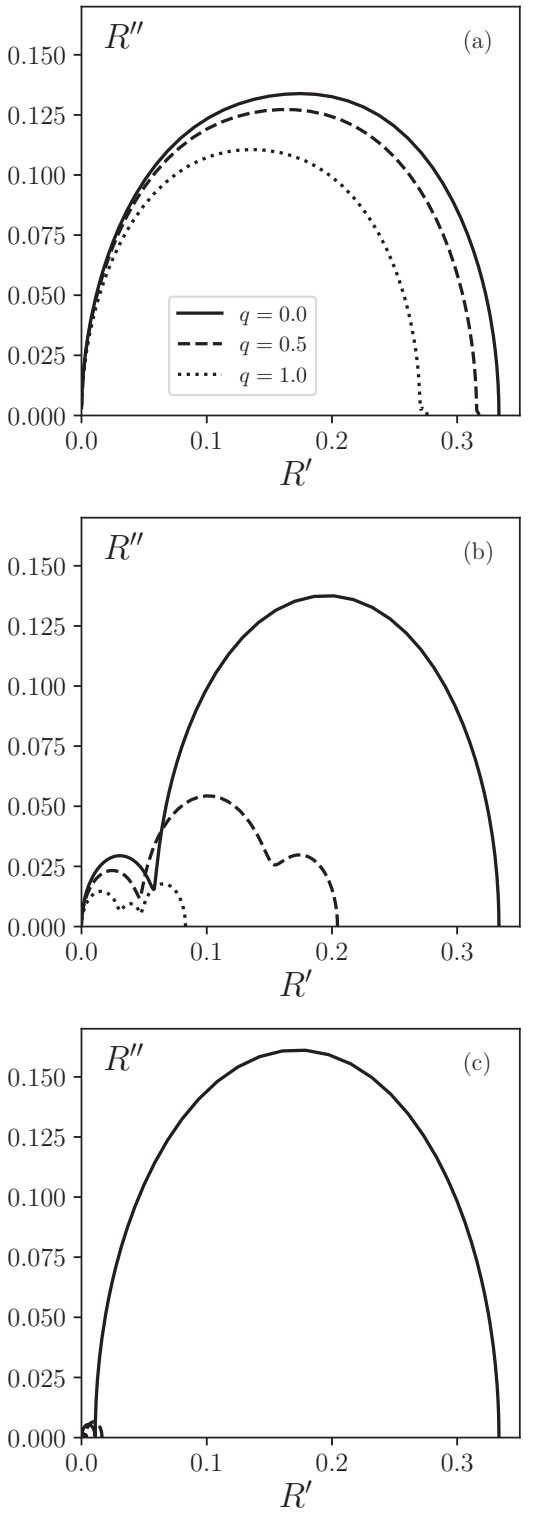

FIG. 2. Cole-Cole diagrams for the response function of a particle with size $x = 1$ (a), 1.5 (b), and 2.5 (c); solid lines: bias field $q_0 = 0$; dashes: $q_0 = 0.5$; dots: $q_0 = 1$. Anisotropy parameter $\kappa = 2$, inverse viscosity $\zeta_0 = 10^{-3}$, surfactant thickness $x_s = 0.5$.

region $\omega\tau_M \lesssim 10^{-1}$) peak of $R''(\omega)$ which is present even at zero bias field matches the combined Brownian rotation of the particle body and the Néel relaxation of the magnetic moment inside it. When the bias field goes up, this maximum shifts to the right to higher frequencies (at a sufficiently strong field this peak merges with the high-frequency one). Lastly, the third additional maximum on the $R''(\omega)$ curve which appears only in the presence of the dc field is associated with the

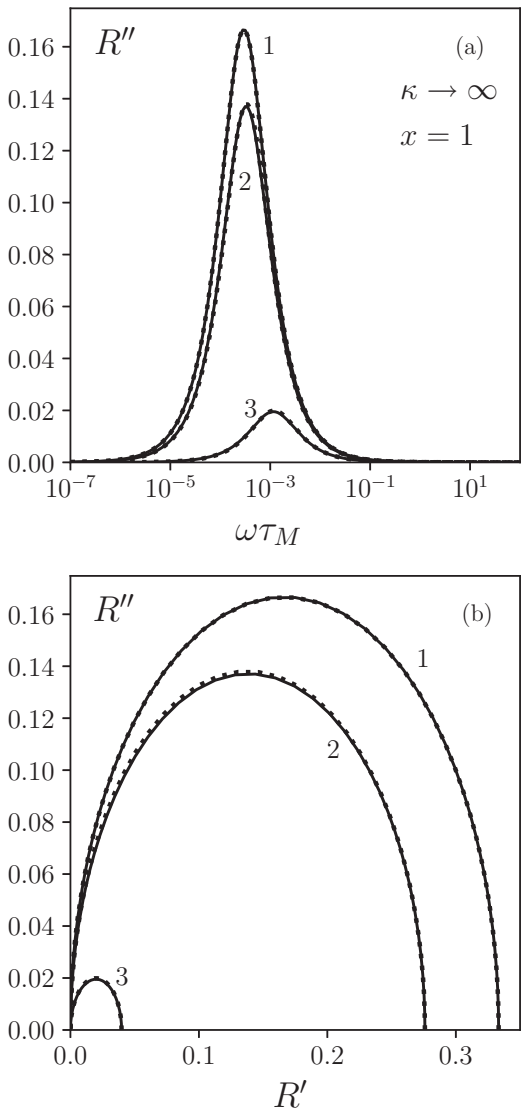

FIG. 3. Frequency dependencies of imaginary parts of the response function (a) and Cole-Cole diagrams (b) for a rigid dipole ($\kappa \to \infty$) of size $x = 1$ for several magnitudes of the bias field: $q_0 = 0$ (curves 1), $q_0 = 1$ (curves 2), and $q_0 = 5$ (curves 3); solid lines: numerical calculation; dots: Eq. (33); inverse viscosity $\zeta_0 = 10^{-3}$, surfactant thickness $x_s = 0.5$.

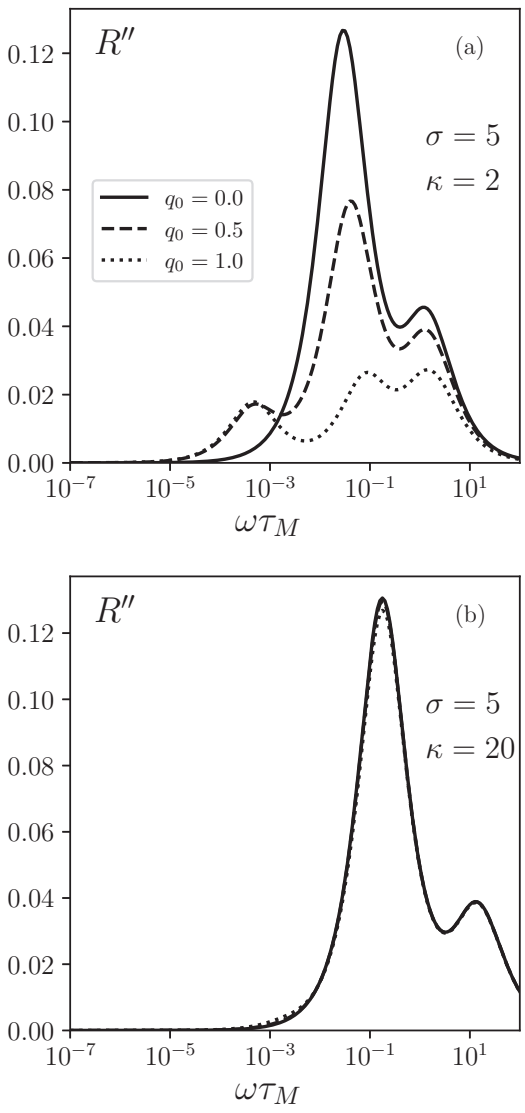

FIG. 4. Frequency dependencies of the imaginary part of the response function for particles with the same ratio of anisotropy energy to thermal one ($\sigma = 5$), but different values of the anisotropy parameter: $\kappa = 2$ (a) and $\kappa = 20$ (b); solid lines: bias field $q_0 = 0$, dashes: $q_0 = 0.5$, dots $q_0 = 1$; inverse viscosity $\zeta_0 = 10^{-3}$; surfactant thickness $x_s = 0.5$.

Brownian rotation of a particle whose intrinsic magnetic state is equilibrium. This peak is, obviously, impossible for mechanically fixed particles because they do not have rotational degrees of freedom.

The case $\sigma \to \infty$ requires a special consideration. In this limit, the magnetic response of a nanoparticle suspended in a fluid can be considered by means of the so-called rigid dipole approximation. This approach does not take into account superparamagnetism of particles at all: it is believed that thermal fluctuations of the angle between magnetic moment of a particle and its anisotropy axis are completely negligible. Thus, comparing results of the full theory and the rigid-dipole approach, one can reveal superparamagnetic effects in the magnetic response of the system. As shown in Fig. 3, for a rigid dipole, the function $R(\omega)$ has two specific features. First, it includes the only maximum in the frequency range $\omega\tau_M \ll 1$ at any values of the bias field q_0. Second, in the range $\omega\tau_M \gtrsim 10^{-1}$, the signal is exactly zero. It is interesting to note that at $q_0 = 0$ the Cole-Cole diagrams for particles with $\sigma \lesssim 1$ and $\sigma \to \infty$ are identical; compare the solid lines in Figs. 2(a) and 3(b).

It is important to emphasize that the disappearance of the internal diffusion of the magnetic moment at $\sigma \to \infty$ does not mean at all that σ is the only parameter whose value determines superparamagnetic peculiarities in response of a suspended particle. This is clearly demonstrated by Fig. 4, where the lines $R''(\omega)$ are shown for particles with the same value of σ but different values of the anisotropy constant: $\kappa = 2$ (a) and $\kappa = 20$ (b). As can be seen, at $\kappa = 2$ application of even a rather weak bias field q_0 significantly changes the

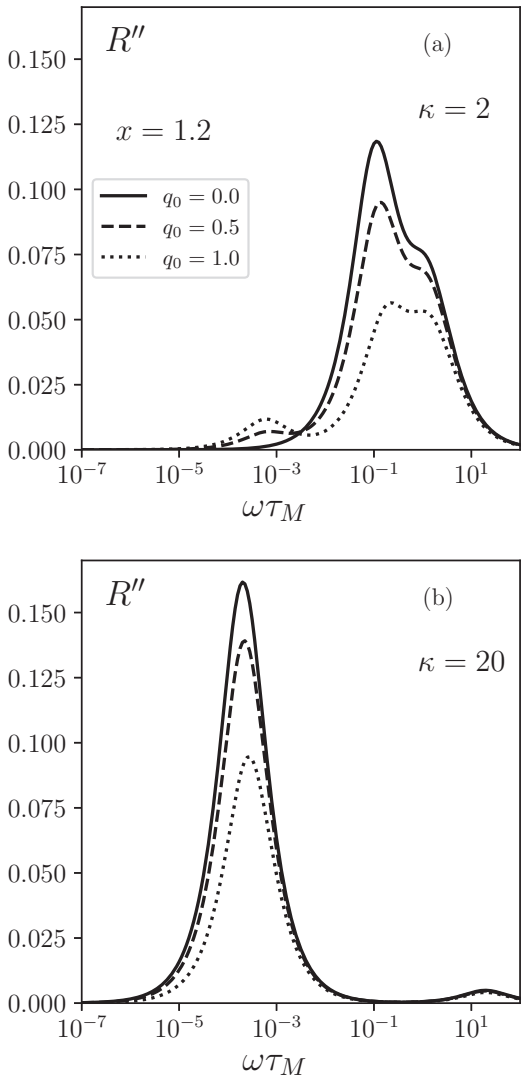

FIG. 5. Frequency dependencies of the imaginary part of the response function for particles of the same size ($x = 1.2$), but with different values of the anisotropy parameter: $\kappa = 2$ (a) and $\kappa = 20$ (b); solid lines: bias field $q_0 = 0$, dashes: $q_0 = 0.5$, dots $q_0 = 1$; inverse viscosity $\zeta_0 = 10^{-3}$, surfactant thickness $x_s = 0.5$.

response function, leading, in particular, to such superparamagnetic effect as appearance of the additional third peak. However, at $\kappa = 20$ the same magnetizing field has almost no effect. The evident reason for this difference is the fact that type of the function R depends not only on the parameter σ but also on the ratio $\xi_0 = \mu H_0/k_B T$. Since $\xi_0 = \sigma\, H_0 M_s/K$, this means that not only value of σ but also the relationship between the applied field H_0 and effective anisotropy field $H_A = K/M_s$ determines specific features of magnetic response of a particle.

Lastly, note that the magnetic response of weakly and strongly anisotropic particles of the same size can be qualitatively different; see Fig. 5.

B. Approximate formula for the response function at $\sigma \gg 1$

The graph of the response function of a rigid dipole ($\kappa \to \infty$, Fig. 3) suggests that $R(\omega)$ can be approximated by a Debye-type expression:

$$R \approx \frac{R_0}{1 + i\omega\tau_B(\xi_0)}, \quad \kappa \to \infty, \tag{33}$$

where static value $R_0 = R(\omega = 0)$ is determined by the derivative of the Langevin function with respect to the bias field,

$$R_0 = \frac{dL(\xi_0)}{d\xi_0} = \frac{1}{\xi_0^2} - \frac{1}{\sinh^2 \xi_0}, \quad L(\xi) = \coth(\xi_0) - \frac{1}{\xi_0}, \tag{34}$$

and relaxation time $\tau_B(\xi_0)$ is inversely proportional to the smallest (in absolute terms) eigenvalue of the kinetic operator $\hat{S}_0$ in the limit $\sigma \to \infty$. In accordance with Ref. [17], this time can be approximately considered equal to

$$\tau_B(\xi_0) = \frac{\xi_0}{L(\xi_0)} \frac{dL(\xi_0)}{d\xi_0}. \tag{35}$$

The results of calculations by Eqs. (33)–(35) are demonstrated by dots in Fig. 3; as can be seen, they are in good agreement with numerical data shown by solid lines.

In the case when $\sigma \gg 1$ but is finite, the spectrum $R''(\omega)$ has exactly two peaks at any magnitude of the bias field. This means the response function $R(\omega)$ comprises at least two Debye-type terms that correspond to qualitatively different relaxation modes. The first one matches Brownian rotation of the particle body accompanied by thermofluctuational transitions of the magnetic moment over the energy barrier. At $\sigma \gg 1$ and $\xi_0 \lesssim \sigma$, the corresponding relaxation time is approximately equal to $\tau_B(\xi_0)$ since the rate of magnetization reversal inside the particle is exponentially small. The second contribution to $R(\omega)$ is delivered by the intrawell modes. At $\sigma \gg 1$, they can roughly be characterized by the precession decay time equal to $(1 + \alpha^2)/\alpha\gamma(2K/M_s + H_0) = \tau_M/(\kappa + q_0/2)$. Then taking into account that the static value R_0 of the response function does not depend on the particle anisotropy (see, e.g., Ref. [18]), one can write

$$R(\omega) \approx \frac{R_0 - \Delta_\kappa}{1 + i\omega\tau_B(\xi_0)} + \frac{\Delta_\kappa}{1 + i\omega\tau_M/(\kappa + q_0/2)}, \quad \sigma \gg 1, \tag{36}$$

where the weight Δ_κ is a function of the parameters σ and ξ. For the case without the biasing, the accurate asymptotics for Δ_κ can be written following Refs. [19,20]:

$$\Delta_\kappa = \frac{1}{3}\left(\frac{1}{\sigma} + \frac{3}{4\sigma^2}\right), \quad \sigma \gg 1, \quad q_0 = 0. \tag{37}$$

In the presence of the magnetizing field, the weight Δ_κ falls down due to orientation ordering of the anisotropy axis of a suspended particle. As a characteristic of the effect, one can use the unperturbed average value $\langle P_2(\boldsymbol{n} \cdot \boldsymbol{f})\rangle_0$ of the second Legendre polynomial that depends on the angle between easy magnetization axis and direction of the bias field. According to Ref. [21], the indicated average is proportional to the second Langevin function $L_2(\xi_0) = 1 - 3L_1(\xi_0)/\xi_0$. When the biasing is absent, $\xi_0 = 0$, the orientation distribution of anisotropy axis is uniform, so $\langle P_2(\boldsymbol{n} \cdot \boldsymbol{f})\rangle_0 = 0$ and $L_2 = 0$. It is therefore reasonable to assume that the weight of the intrawell modes in the presence of the dc field can be represented as $\Delta_\kappa = \Delta_\kappa(\xi_0 = 0)\,[1 + g(\sigma)L_2(\xi_0)]$. The unknown

function $g(\sigma)$ is found by comparison of this approximation with numerical data and minimization of the corresponding variance; the result looks like

$$\Delta_\kappa = \frac{1}{3}\left(\frac{1}{\sigma}+\frac{3}{4\sigma^2}\right)\left[1-\left(1+\frac{11}{5\sigma}-\frac{71}{5\sigma^2}\right)L_2(\xi_0)\right]. \quad (38)$$

Expressions Eqs. (36)–(38) agree well with numerical data at $\sigma \gtrsim 15$, compare, for example, points (approximate calculation) and solid lines (numerical data) in Fig. 6. The derivation performed does not, certainly, pretend to be rigorous. Nevertheless, the found relations, on the one hand, are useful for a systematization of numerical data, and on the other, are very helpful in studying limiting cases.

IV. DYNAMIC MAGNETIC SUSCEPTIBILITY OF A POLYDISPERSE ENSEMBLE OF PARTICLES

Let us now consider ensembles of suspended particles whose diameters are not necessarily the same. Generally, the distribution of particle sizes depends on a method used to prepare a sample. However, in most cases, the entire set of particle diameters can be satisfactorily specified by a two-parameter function. Usually, either lognormal (see, e.g., Ref. [22]) or gamma distribution (see, e.g., Ref. [23]) are involved but the choice between them is not fundamental. For the given function ρ, the dynamic susceptibility of a polydisperse ensemble of particles is delivered by Eqs. (26) and (30). Hereinafter, in those cases where results can be obtained only numerically, the gamma distribution

$$\rho(x) = \frac{x^{\alpha-1}e^{-x/x_0}}{x_0^\alpha \Gamma(\alpha)} \quad (39)$$

is adopted; parameters x_0 and α determine the average value $\langle x\rangle$ and the relative standard deviation $\delta = \sqrt{\langle (x-\langle x\rangle)^2\rangle}/\langle x\rangle$:

$$x_0 = \langle x\rangle \delta^2, \quad \alpha = \frac{1}{\delta^2}. \quad (40)$$

The static magnetic susceptibility $\tilde\chi_0 = \tilde\chi(\omega = 0)$ is found as

$$\tilde\chi_0 = \int_0^\infty x^6\,\rho(x)\,R(\omega=0;\,x)dx = \int_0^\infty x^6\,\rho(x)\left.\frac{dL(\xi_0)}{d\xi_0}\right|_{\xi_0=qx^3} dx. \quad (41)$$

If the bias field is weak and for most particles in an ensemble the parameter $\xi_0 = q_0x^3 \lesssim 2$, then $R(\omega=0;\,x)\approx 1/3 - q^2x^6/15$, and

$$\tilde\chi_0 \approx \frac{1}{3}\langle x^6\rangle - \frac{q^2}{15}\langle x^{12}\rangle. \quad (42)$$

On the contrary, if the magnetizing field is strong and for most particles $\xi_0 = q_0x^3 \gtrsim 2$, then $R(\omega=0;\,x)\approx 1/q^2x^6$, and

$$\tilde\chi_0 \approx 1/q^2 \quad (43)$$

for any size distribution $\rho(x)$.

In contrast to the static one, the dynamic magnetic response of a particle suspended in a fluid depends on the anisotropy parameter κ as well. Since for the given field q_0 it can be qualitatively different for particles with strong ($\kappa \gg 1$) and weak or moderate ($\kappa \sim 1$) anisotropy, it makes sense to consider two types of ensembles separately.

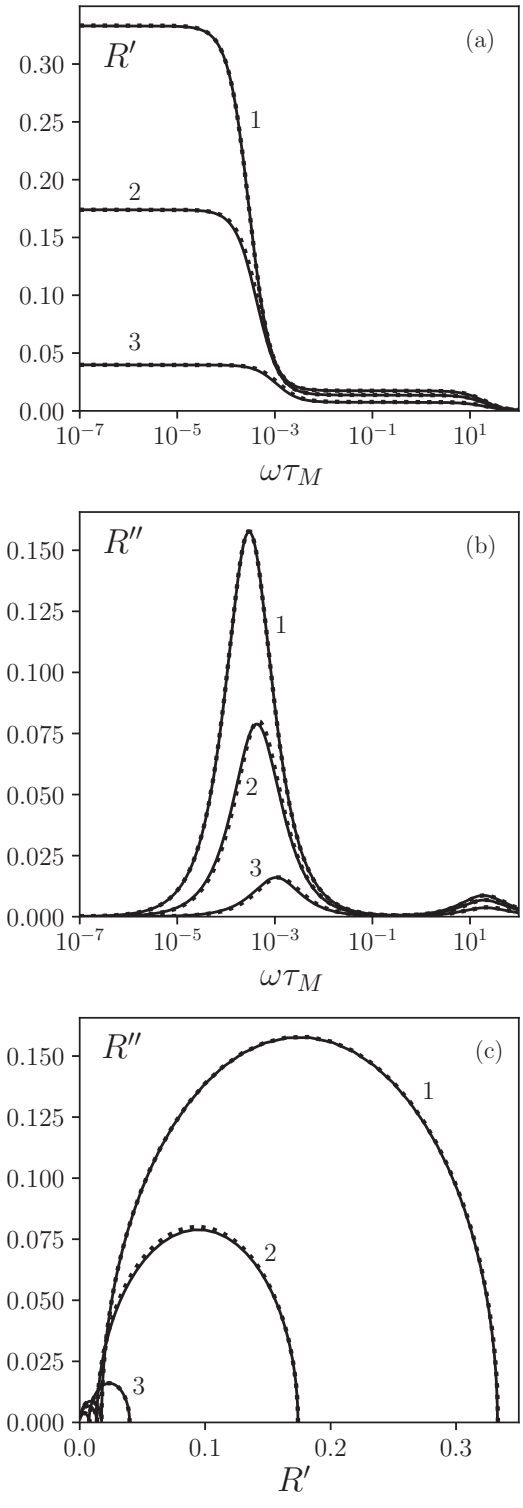

FIG. 6. Frequency dependencies of real (a) and imaginary (b) parts of the response function and the corresponding Cole-Cole diagrams (c) for the particle with size $x = 1$ and anisotropy parameter $\kappa = 20$ at different values of the bias field: $q_0 = 0$ (lines 1), 2 (lines 2) and 5 (lines 3). Solid lines: numerical calculations; dots: approximate formula Eq. (36); inverse viscosity $\zeta_0 = 10^{-3}$, surfactant thickness $x_s = 0.5$.

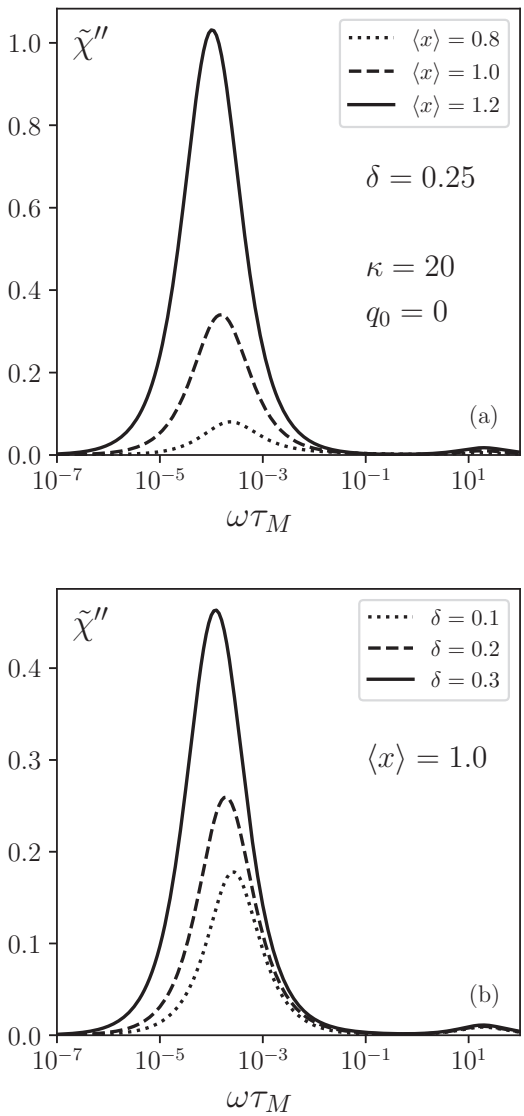

FIG. 7. Frequency dependencies of the imaginary part of the dynamic magnetic susceptibility of polydisperse ensembles of strongly anisotropic (parameter $\kappa = 20$) particles in zero bias field ($q_0 = 0$); inverse viscosity $\zeta_0 = 10^{-3}$, surfactant thickness $x_s = 0.5$. (a) Different curves correspond to different values of the average particle diameter: dots $\langle x\rangle = 0.8$, dashes $\langle x\rangle = 1$, solid lines $\langle x\rangle = 1.2$; standard deviation $\delta = 0.2$. (b) Different curves correspond to different values of the standard deviation: dots $\delta = 0.1$, dashes $\delta = 0.2$, solid lines $\delta = 0.3$; average diameter $\langle x\rangle = 1$.

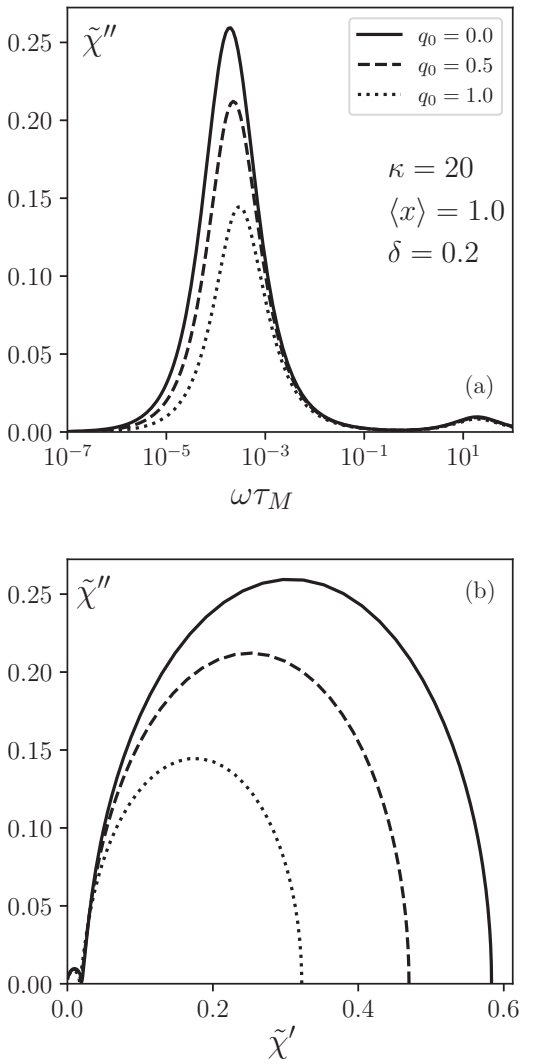

FIG. 8. Frequency dependencies of imaginary part of the dynamic magnetic susceptibility (a) and Cole-Cole diagrams (b) of the polydisperse ensemble of strongly anisotropic (parameter $\kappa = 20$) particles at different values of the bias field: $q_0 = 0$ (solid lines), $q_0 = 0.5$ (dashes), $q_0 = 1$ (dots); average diameter $\langle x\rangle = 1.0$, standard deviation $\delta = 0.2$, inverse viscosity $\zeta_0 = 10^{-3}$, surfactant thickness $x_s = 0.5$.

1. Ensemble of particles with strong magnetic anisotropy

In Fig. 7, one can see frequency dependencies of the imaginary component of the dynamic magnetic susceptibility (absorption lines) of polydisperse ensembles of particles with anisotropy parameter $\kappa = 20$ in the case $q_0 = 0$ (no bias field). The presented absorption spectra include two maxima: low-frequency ($\omega\tau_M \ll 1$) and high-frequency ($\omega\tau_M \sim 1$), while in the midfrequency region ($\omega\tau_M \sim 0.1$) values of $\tilde{\chi}''(\omega)$ are close to zero. The reason for such a behavior is quite clear: if $\kappa \gg 1$ (and the average size $\langle x\rangle \sim 1$ as in Fig. 7), then for most particles, the parameter $\sigma \gtrsim 10$ and the response function corresponds to Fig. 1(c). As expected, a growth of average diameter [see Fig. 7(a)] or width of the size distribution [Fig. 7(b)] leads to an increase in the signal and to a shift of the left maximum to region of lower frequencies. Both of these effects are obviously explained by following: (i) the larger the particle, the greater its contribution to the magnetic susceptibility, see Eq. (30); and (ii) the larger the particle, the lower the frequency of the left absorption maximum; see Fig. 1. The bias field is expected to reduce the height of the low-frequency absorption maximum and shift it to the right; see Fig. 8(a). With that, its effect on the high frequency ($\omega\tau_M \gtrsim 10^{-1}$) response of the system is rather slight. It is especially clear from the Cole-Cole diagrams [Fig. 8(b)]: in the area near origin, they are almost the same for all selected values q_0.

For the case under consideration, some interesting conclusions about superparamagnetic effects can be directly drawn using Eq. (36) for the response function of a particle. In

the range $\omega\tau_M \lesssim 10^{-1}$, the second term in (36) is virtually frequency independent and the response function is approximately equal to

$$R(\omega) = \frac{R_0 - \Delta_\kappa}{1 + i\omega\tau_B(\xi_0)} + \Delta_\kappa = \left(\frac{R_0}{1+\omega^2\tau_B^2(\xi_0)} + \Delta_\kappa \frac{\omega^2\tau_B^2(\xi_0)}{1+\omega^2\tau_B^2(\xi_0)}\right) - i\left(\frac{\omega\tau_B(\xi_0) R_0}{1+\omega^2\tau_B^2(\xi_0)} - \Delta_\kappa \frac{\omega\tau_B(\xi_0)}{1+\omega^2\tau_B^2(\xi_0)}\right). \quad (44)$$

Therefore, the real $\tilde\chi'$ and imaginary $\tilde\chi''$ parts of the dynamic magnetic susceptibility $\tilde\chi = \tilde\chi' - i\tilde\chi''$ of the ensemble are

$$\tilde\chi' = \tilde\chi'_{\rm rd} + \int_0^\infty \Delta_\kappa \frac{\omega^2\tau_B^2(\xi_0)}{1+\omega^2\tau_B^2(\xi_0)} x^6\rho(x)\,dx,$$
$$\tilde\chi'' = \tilde\chi''_{\rm rd} - \int_0^\infty \Delta_\kappa \frac{\omega\tau_B(\xi_0)}{1+\omega^2\tau_B^2(\xi_0)} x^6\rho(x)\,dx, \quad (45)$$

where the terms

$$\tilde\chi'_{\rm rd} = \int_0^\infty \frac{R_0}{1+\omega^2\tau_B^2(\xi_0)} x^6\rho(x)\,dx \quad \text{and}$$
$$\tilde\chi''_{\rm rd} = \int_0^\infty \frac{\omega\tau_B(\xi_0) R_0}{1+\omega^2\tau_B^2(\xi_0)} x^6\rho(x)\,dx \quad (46)$$

determine result in the rigid-dipole approximation. The integrals in Eq. (45) are strictly positive; this means that in the specified frequency region, diffusion of the magnetic moment inside particles always leads to an increase in real component of the dynamic susceptibility of the system and to a decrease in its imaginary one. With that, the integrals are proportional to the frequency ω of the exciting field and, therefore, their contribution to $\tilde\chi$ effectively down when ω diminishes. As the latter tends to zero, the outcome of calculations is completely independent of anisotropy of particles and the rigid-dipole model gives the accurate result.

In the zero bias field, the weight of the intrawell modes is $\Delta_\kappa = 1/(3\kappa x^3) + 1/(4\kappa^2 x^6)$ and the expressions take the form

$$\tilde\chi' = \tilde\chi'_{\rm rd} + \int_0^\infty \frac{\omega^2\tau_B^2}{1+\omega^2\tau_B^2}\left(\frac{x^3}{3\kappa} + \frac{1}{4\kappa^2}\right)\rho(x)\,dx, \quad \tilde\chi'' = \tilde\chi''_{\rm rd} - \int_0^\infty \frac{\omega\tau_B}{1+\omega^2\tau_B^2}\left(\frac{x^3}{3\kappa} + \frac{1}{4\kappa^2}\right)\rho(x)\,dx, \quad (47)$$

$$\tilde\chi'_{\rm rd} = \frac{1}{3}\int_0^\infty \frac{1}{1+\omega^2\tau_B^2} x^6\rho(x)\,dx, \quad \tilde\chi''_{\rm rd} = \frac{1}{3}\int_0^\infty \frac{\omega\tau_B}{1+\omega^2\tau_B^2} x^6\rho(x)\,dx. \quad (48)$$

As $\tau_B = \tau_M\,(x + x_s)^3/\zeta_0$, in the region of low frequencies $\omega\tau_M/\zeta_0 \ll 1$, the following estimates are valid:

$$\tilde\chi' \approx \tilde\chi'_{\rm rd} + \left(\frac{\omega\tau_M}{\zeta_0}\right)^2 \cdot \left(\frac{\langle x^9\rangle}{3\kappa} + \frac{\langle x^6\rangle}{4\kappa^2}\right), \quad \tilde\chi'' \approx \tilde\chi''_{\rm rd} - \left(\frac{\omega\tau_M}{\zeta_0}\right) \cdot \left(\frac{\langle x^6\rangle}{3\kappa} + \frac{\langle x^3\rangle}{4\kappa^2}\right), \quad (49)$$

$$\tilde\chi'_{\rm rd} \approx \frac{\langle x^6\rangle}{3}, \quad \tilde\chi''_{\rm rd} \approx \left(\frac{\omega\tau_M}{\zeta_0}\right)\frac{\langle (x+x_s)^3 \cdot x^6\rangle}{3}, \quad (50)$$

which confirm that at $\omega\tau_M \ll \zeta_0$ superparamagnetic effects are neglible.

In the frequency range $\zeta_0 \lesssim \omega\tau_M \lesssim 10^{-1}$, Eqs. (47)–(48) are approximately reduced to

$$\tilde\chi' \approx \tilde\chi'_{\rm rd} + \frac{\langle x^3\rangle}{3\kappa} + \frac{1}{4\kappa^2}, \quad \tilde\chi'' \approx \tilde\chi''_{\rm rd} - \frac{\zeta_0}{\omega\tau_M}\left(\frac{1}{3\kappa} + \frac{1}{4\kappa^2}\int_0^\infty \frac{\rho(x)}{(x+x_s)^3}\,dx\right), \quad (51)$$

$$\tilde\chi'_{\rm rd} \approx \frac{1}{3}\cdot\left(\frac{\zeta_0}{\omega\tau_M}\right)^2 \cdot \left\langle\left(\frac{x}{x+x_s}\right)^6\right\rangle, \quad \tilde\chi''_{\rm rd} \approx \frac{1}{3}\cdot\left(\frac{\zeta_0}{\omega\tau_M}\right)\cdot\left\langle\left(\frac{x^2}{x+x_s}\right)^3\right\rangle. \quad (52)$$

As seen, at any particle-size distribution the adjustment for the internal diffusion of the magnetic moment goes to zero only at $\kappa \to \infty$. Note also that the specified correction is not diminshed with an enhancement of particle sizes (which entails growth of values of the anisotropy parameter σ) but in the opposite rises.

Let us consider the high-frequency response of the system. In the range $\omega\tau_M \gtrsim 10^{-1}$, the first term in Eq. (36) vanishes, so the dynamic magnetic susceptibility of the ensemble is approximately equal to

$$\tilde\chi \approx \frac{1}{1 + i\omega\tau_M/(\kappa + q_0/2)}\int_0^\infty \Delta_\kappa\, x^6\rho(x)\,dx, \quad \omega\tau_M \gtrsim 10^{-1}. \quad (53)$$

In the absence of the bias field, it reduces to

$$\tilde\chi = \frac{1}{1 + i\omega\tau_M/\kappa}\int_0^\infty \left(\frac{x^3}{3\kappa} + \frac{1}{4\kappa^2}\right)\rho(x)dx = \left[\frac{1}{4\kappa^2} + \frac{\langle x^3\rangle}{3\kappa}\right]\frac{1}{1 + i\omega\tau_M/\kappa}, \quad \omega\tau_M \gtrsim 10^{-1}. \quad (54)$$

Thus, at finite values of κ, the high-frequency response is nonzero at any particle-size distribution due to the intrawell relaxation of the magnetic moment inside particles.

The drawn conclusions are entirely consistent with the computational results. In Fig. 9, one can see Cole-Cole diagrams of two ensembles with different values of the average

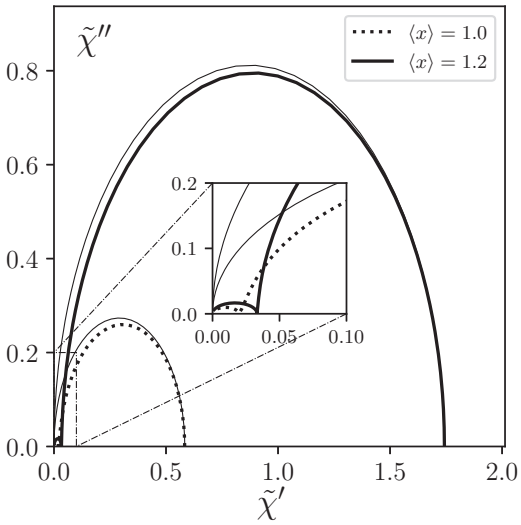

FIG. 9. Cole-Cole diagrams of polydisperse ensembles of particles with anisotropy parameter $\kappa = 20$ for different values of the average diameter: $x = 1$ (dots) and $x = 1.2$ (thick solid line); thin solid lines correspond to the rigid dipole approximation; relative standard deviation $\delta = 0.2$, viscosity parameter $\zeta_0 = 10^{-3}$, surfactant thickness $x_s = 0.5$—the biasing is absent.

particle size (the relative width of the distribution is the same). Thin solid lines demonstrate output of the rigid-dipole approximation—they strictly cross the origin; thick solid line and dashes are obtained by the full numerical procedure. It is clear that at high frequencies ($\omega\tau_M \gtrsim 10^{-1}$, the corresponding sections of the diagrams are enlarged in the inset), both in-phase and out-of-phase components of the magnetic response are higher for the system with the larger average size of particles. In frequency region $\omega\tau_M/\zeta_0 \gtrsim 1$ (parts to the left of the maximum point of the diagrams), an increase in $\langle x\rangle$ also does not lead to the disappearance of the superparamagnetic contribution. On the contrary, two lines—found by the full calculation and by the rigid-dipole method—move somewhat away from each other, mainly due to an increase in the in-phase component of the susceptibility. However, in the low-frequency region (sections to the right of the maximum point of the diagrams) the specified lines practically coincide.

2. Moderate and weak magnetic anisotropy

For polydisperse suspensions of particles with anisotropy parameter $\kappa \sim 1$, a set of possible types of the magnetic response is expected to be more diverse. Typical options are illustrated in Fig. 10, where the absorption lines of the system with $\kappa = 5$ are presented for several values of the average particle diameter and the bias field. As can be seen, for the ensemble of relatively small particles with $\langle x\rangle = 0.6$ [case (a)], the frequency sweep of $\tilde{\chi}''$ includes the only peak in the high-frequency range $\omega\tau_M \gtrsim 10^{-1}$ when $q_0 = 0$ and the biasing leads to an additional maximum at $\omega\tau_M \sim \zeta_0$. For the ensemble with $\langle x\rangle = 0.8$ [case (b)], there are two absorption peaks in the region $\omega\tau_M \gtrsim 10^{-2}$ (see solid line) and due to the biasing the third maximum can appear at frequency $\omega\tau_M \sim \zeta_0$ (see dashes). For $\langle x\rangle = 1$ [case (c)], the spectrum, as shown by the solid line, actually has three maxima even without dc field; however, application of the latter can increase resolution of the peaks, see dashes. Finally, if an ensemble consists of sufficiently large particles [relatively big average size and/or distribution width, case (d)], then the absorption line has exactly two peaks: low- and high-frequency ones. A spectrum of the same shape is typical for particles with strong anisotropy, compare, for example, Figs. 8(a) and 10(d). However, there is a significant difference between two situations: at $\kappa \gg 1$ the bias field $q_0 \sim 1$ has no noticeable effect on the magnetic response of the system in the range $\omega\tau_M \gtrsim 10^{-1}$ [in Fig. 8(a), all curves in the specified band are close to each other] but at $\kappa \sim 1$ the influence of the biasing is significant (lines at different q_0 are diverse). Nonetheless, in the study of magnetic resonance, the bias field can play a crucial role even for a suspension of strongly anisotropic particles [24].

As shown in Fig. 10, the magnetizing field in most cases reduces the response of the system and the effect is stronger the larger particles in an ensemble. However, if for a substantial part of particles condition $\sigma \lesssim \sigma_*$ is met and their response function matches Figs. 1(a), 1(b) and 2(a), 2(b), then the dc field can increase out-of-phase component of the susceptibility in the low-frequency region and cause appearance of the additional absorption peak at $\omega\tau_M \sim \zeta_0$, see Fig. 10(a). Let us make somewhat rough estimates for values of $\langle x\rangle$ and δ at which this effect is possible. According to Eq. (30), the contribution of each particle to the total magnetic response of the system is determined by the combination $x^6\rho(x)$. Therefore, it is reasonable to introduce the normalized function

$$\beta(x) = A\,x^6\rho(x), \quad A^{-1} = \int_0^\infty x^6\rho(x)\,dx, \tag{55}$$

such that

$$\tilde{\chi}(\omega) = \int_0^\infty \beta(x) R(\omega; x)\,dx. \tag{56}$$

If particle sizes in an ensemble obey Eq. (39), then

$$\beta(x) = \frac{x^{\alpha+5} e^{-x/x_0}}{x_0^{\alpha+6}\,\Gamma(\alpha+6)}, \quad \int_0^\infty \beta(x)\,dx = 1. \tag{57}$$

Distribution Eq. (57) has the single maximum at $x_m = (\alpha + 5)\,x_0$ and the quantity

$$D_\beta = \langle x^2\rangle_\beta - \langle x\rangle_\beta^2 = x_0^2\,(\alpha+6),$$
$$\langle \ldots\rangle_\beta = \int_0^\infty (\ldots)\beta(x)\,dx, \tag{58}$$

provides an estimate for its width. In a bias field, the imaginary part of the response function R of a particle can acquire the additional low-frequency peak only if $\sigma \lesssim \sigma_*$. In a polydisperse ensemble the predominant part of the magnetic signal comes from the particles whose magnetic diameter does not exceed value $x_m + \sqrt{D_\beta}$; therefore, making an estimation, it is reasonable to assume that appearance of the extra maximum at $\omega\tau_M \sim \zeta_0$ is possible if

$$x_m + \sqrt{D_\beta} \lesssim x_*, \quad x_* = \sqrt[3]{\frac{\sigma_*}{\kappa}}. \tag{59}$$

Substituting the expressions for x_m and $\sqrt{D_\beta}$ and taking into account that at $5.5 \lesssim \sigma_* \lesssim 17$ approximately $\sqrt[3]{\sigma_*} \approx 2$, one

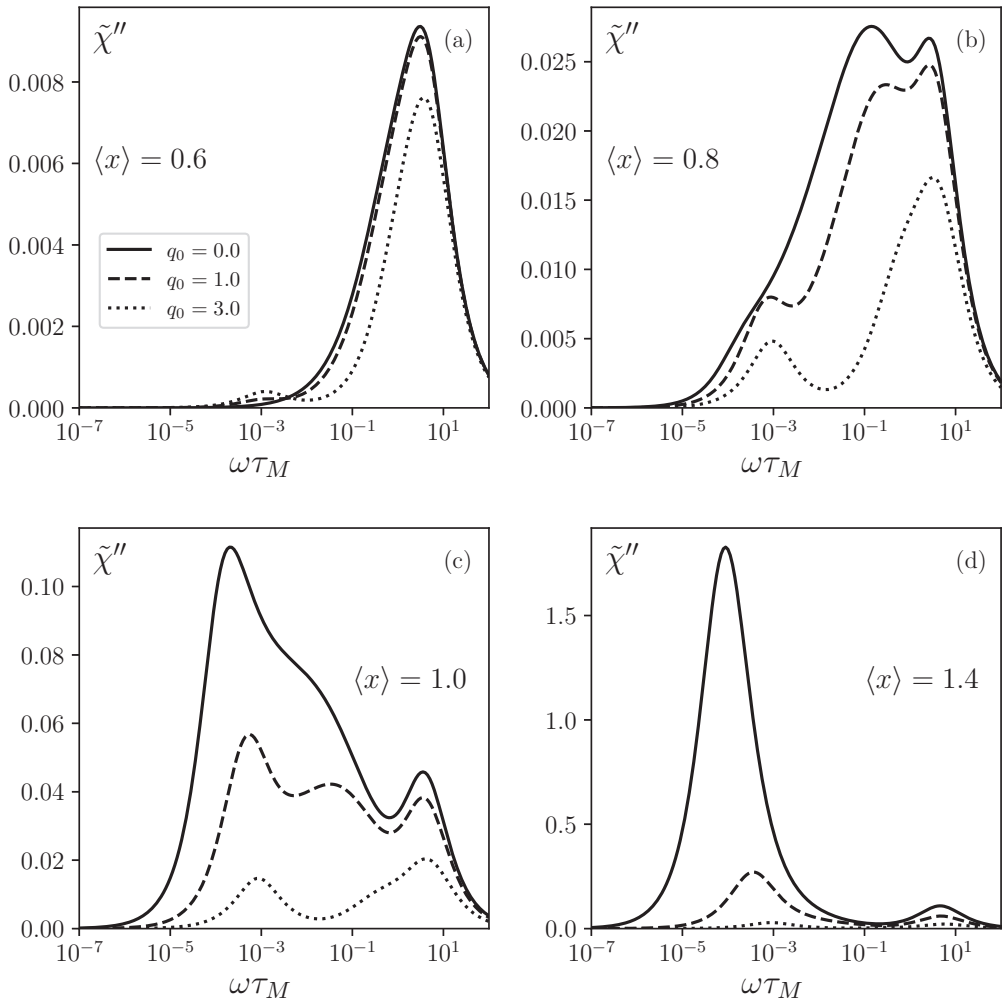

FIG. 10. Absorption lines of polydisperse ensembles of moderately anisotropic (parameter $\kappa = 5$) superparamagnetic nanoparticles suspended in a fluid, the average magnetic diameter $\langle x\rangle = 0.6$ (a), $\langle x\rangle = 0.8$ (b), $\langle x\rangle = 1$ (c), and $\langle x\rangle = 1.4$ (d); solid lines: bias field $q_0 = 0$, dashes: $q_0 = 1$, dots: $q_0 = 3$; relative distribution width $\delta = 0.2$, viscosity parameter $\zeta_0 = 10^{-3}$, surfactant thickness $x_s = 0.5$.

obtains the appropriate restriction

$$\langle x\rangle \lesssim \frac{2}{\sqrt[3]{\kappa}} \frac{1}{1 + 5\delta^2 + \delta + 3\delta^3} \tag{60}$$

on parameters $\langle x\rangle$ and δ of the particle-size distribution. Despite simplicity and roughness of the assessment, it agrees quite well with the numerical data. For example, with $\kappa = 5$ and $\delta = 0.2$ the average diameter must meet inequality $\langle x\rangle \lesssim 0.82$ that is in accordance with Fig. 10.

In a similar way, one can formulate an approximate condition for $\langle x\rangle$ and δ under which absorption spectrum of the system has only two peaks [low- and high-frequency as in Fig. 10(d) and also in Figs. 7 and 8]. Such a situation is realized when the overwhelming contribution to the magnetic response comes from particles with $\sigma \gtrsim \sigma_*$. The appropriate inequality looks like $x_m - \sqrt{D_\beta} \gtrsim x_*$ or, in terms of $\langle x\rangle$ and δ,

$$\langle x\rangle \gtrsim \frac{2}{\sqrt[3]{\kappa}} \frac{1}{1 + 5\delta^2 - \delta - 3\delta^3}. \tag{61}$$

For example, for $\kappa = 20$ and $\delta = 0.2$ it gives $\langle x\rangle \gtrsim 0.7$, and for $\kappa = 5$ and $\delta = 0.2$: $\langle x\rangle \gtrsim 1.2$. Results in Figs. 7, 8, and 10 are consistent with these estimates. If Eq. (61) is satisfied, then formulas obtained in Sec. IV 1 are permissible for approximate calculations even at $\kappa \sim 1$.

Note that in sufficiently strong dc fields (q_0 is several units or more), absorption spectrum of a suspension becomes two-peak regardless of particle diameters; see dots in Fig. 10.

V. DISCUSSION

From the above estimates, it follows that, in principle, at every finite value of the anisotropy parameter $\kappa = K/M_s^2$ the absorption spectrum of a suspension may be of any type from Fig. 10. If the particle-size distribution obeys Eq. (60), then absorption lines look like those in Fig. 10(a) or Fig. 10(b); if the inequality Eq. (61) is satisfied, then the lines match Fig. 10(d) (or Figs. 7 and 8); in other cases, the absorption spectrum is of type Fig. 10(c). However, for a suspension of particles with strong magnetic anisotropy ($\kappa \gg 1$), one should expect that with a standard synthesis technique used, the dynamic magnetic susceptibility follows Fig. 10(d) (or Figs. 7 and 8). A vivid example of strongly anisotropic nanoparticles is the cobalt ferrite ones; typically, the effective anisotropy constant for them is no less than $K \approx 3 \times 10^6$ erg/cm^3, and so,

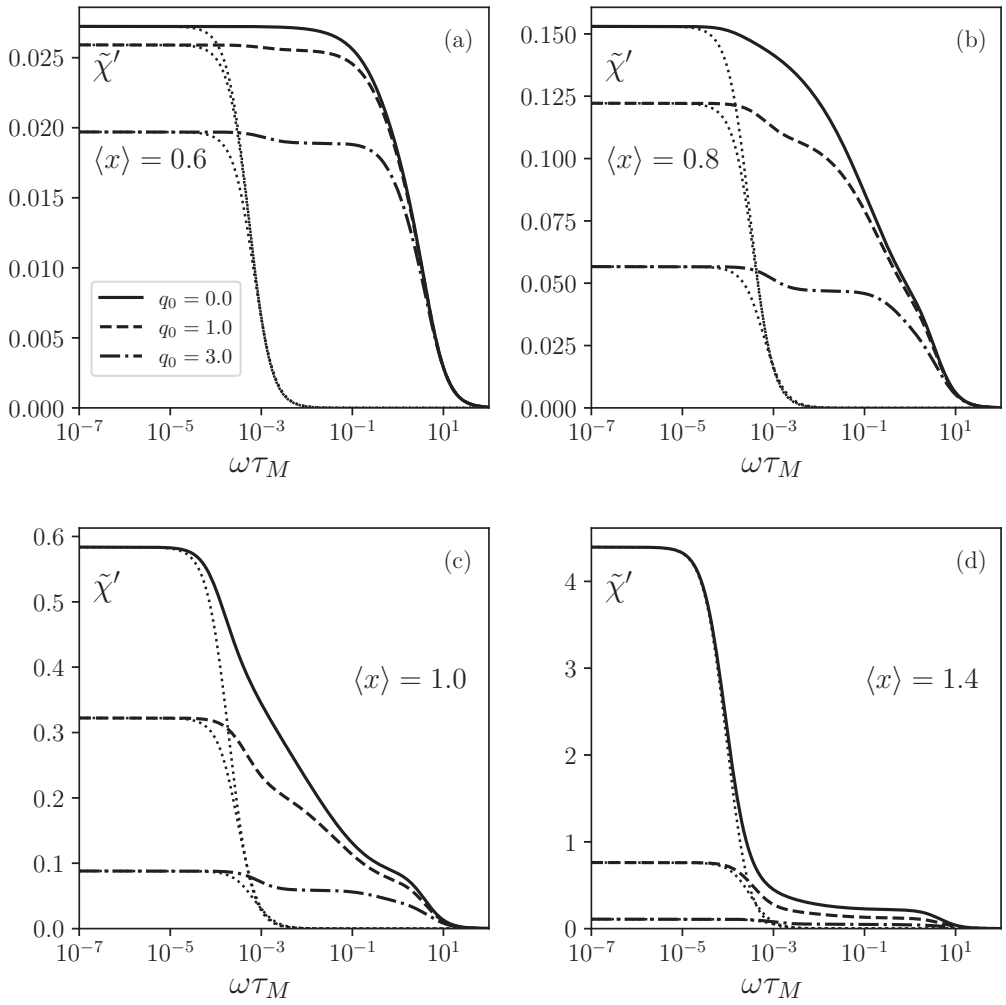

FIG. 11. Frequency dependencies of the real part of the dynamic magnetic susceptibility of nanoparticles, suspended in a fluid, at different values of the average diameter (they are the same as in Fig. 10): $\langle x\rangle = 0.6$ (a), $\langle x\rangle = 0.8$ (b), $\langle x\rangle = 1$ (c), and $\langle x\rangle = 1.4$ (d); solid lines correspond to the the bias field $q_0 = 0$, dashes: $q_0 = 1$, dash-dots: $q_0 = 3$; dots show the corresponding results found in the rigid dipole approximation. Relative distribution width $\delta = 0.2$, viscosity parameter $\zeta_0 = 10^{-3}$, surfactant thickness $x_s = 0.5$.

the parameter $\kappa \gtrsim 20$. In such a case, the condition Eq. (60) gives $\langle x\rangle \lesssim 0.7$, or in dimension units, $\langle d\rangle \lesssim 5$ nm, which is not easy to fulfill.

Further, one may conclude that superparamagnetic effects are always expected in the magnetic response of real suspensions of nanoparticles. To summarize, let us compare results for an ensemble of particles with a finite value of anisotropy parameter κ and for rigid dipoles ($\kappa \to \infty$). Frequency dependencies of the real and imaginary components of the dynamic magnetic susceptibility for both systems (with the same disperse composition) are demonstrated by Figs. 11 and 12, correspondingly. It can be seen that a common superparamagnetic effect is the nonzero magnetic response in the range $10^{-2} \lesssim \omega\tau_M \lesssim 10^3$. It appears for two reasons. The first one is the intrawell relaxation with reference time $\sim\tau_M$; it is inherent for any nanoparticle with a finite value of anisotropy constant. Another reason is contribution of the Néel relaxation mode from those particles in an ensemble whose anisotropy parameter $\sigma \lesssim 5$ (for them, the left absorption peak is located rather close to the specified frequency band). An increase in the proportion of large particles and corresponding growth of the average ratio between anisotropy energy and thermal energy does not suppress this effect. Conversely, according to Eqs. (51) and (54), the dynamic magnetic susceptibility in the specified frequency band even raises with the enlargement of particles (see also solid lines in Figs. 11 and 12).

If particles are large enough and/or strongly anisotropic and the ensemble satisfies the condition Eq. (61), then at other frequencies ($\omega\tau_M \lesssim 10^{-1}$) the internal diffusion of the magnetic moment causes just quantitative changes, see Figs. 11(d) and 12(d). The corresponding corrections diminish with the frequency reduction, becoming negligible at $\omega\tau_M \ll \zeta_0$; see Eq. (49). However, for an ensemble of relatively small particles, superparamagnetic fluctuations, as shown in Figs. 11(a)–11(c) and 12(a)–12(c), can lead as well to qualitative modifications of the spectra $\tilde{\chi}'(\omega)$ and $\tilde{\chi}''(\omega)$ in any frequency range.

Note that regardless of the polydispersity characteristics, the real component of the dynamic magnetic susceptibility of superparamagnetic particles is always greater than that of rigid dipoles: $\tilde{\chi}' > \tilde{\chi}'_{\rm rd}$. For the imaginary part of the susceptibility in the range $\omega\tau_M \lesssim \zeta_0$, the situation is inverse:

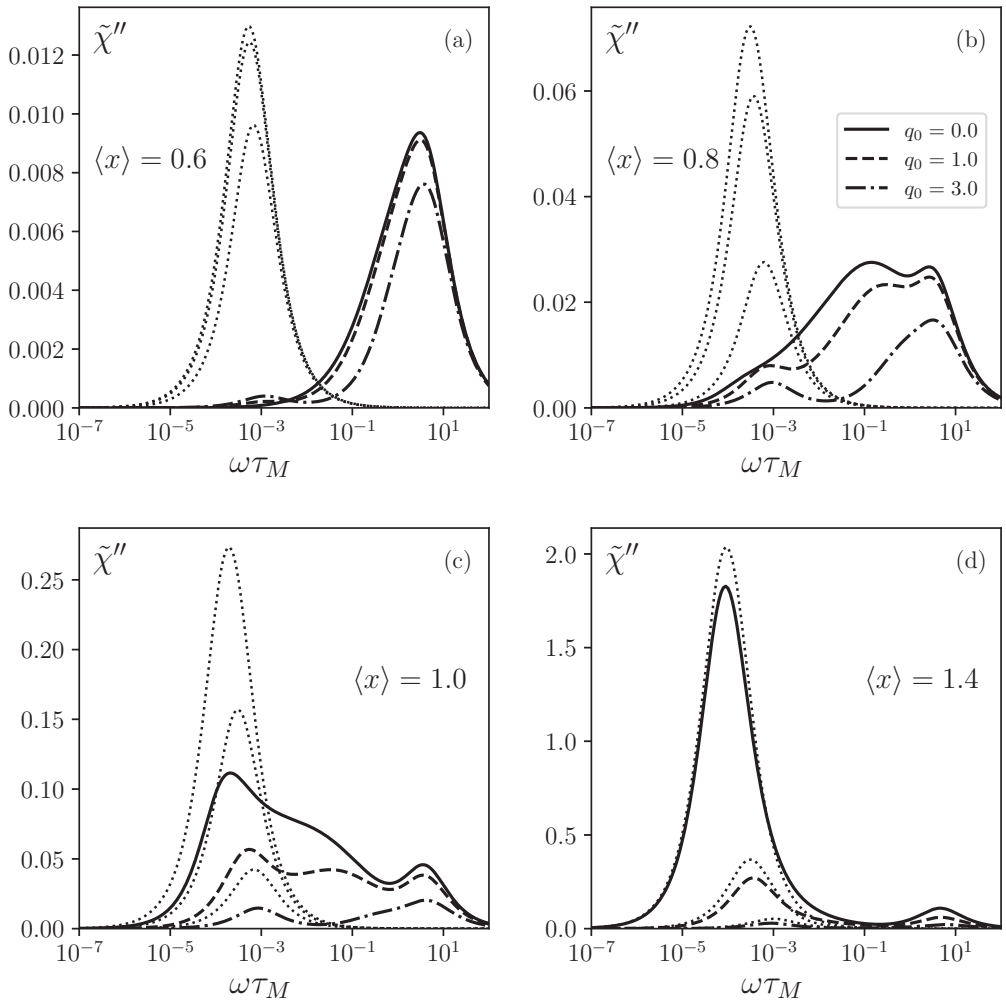

FIG. 12. Frequency dependencies of imaginary part of the dynamic magnetic susceptibility of nanoparticles, suspended in a fluid, at different values of the average diameter (they are the same as in Fig. 10): $\langle x\rangle = 0.6$ (a), $\langle x\rangle = 0.8$ (b), $\langle x\rangle = 1$ (c), and $\langle x\rangle = 1.4$ (d); solid lines correspond to the bias field $q_0 = 0$, dashes: $q_0 = 1$, dash-dots: $q_0 = 3$; dots show the corresponding results found in the rigid dipole approximation.

$\tilde{\chi}'' < \tilde{\chi}''_{\rm rd}$. The interval $\zeta_0 \lesssim \omega\tau_M \lesssim 10^{-1}$ requires a special consideration. Therein, as Fig. 12 demonstrates, any case is possible: superparamagnetism of particles may lead both to a decrease or an increase in $\tilde{\chi}''$. However, it follows from the numerical data that $\tilde{\chi}'' < \tilde{\chi}''_{\rm rd}$ definitely when for most particles the parameter $\sigma \gtrsim 20$ [that is, by analogy with (61), the inequality $\langle x\rangle(1 + 5\delta^2 - \delta - 3\delta^3) \gtrsim \sqrt[3]{20/\kappa}$ is fulfilled] and the relations Eq. (45) are valid. Also, in such a case

$$\frac{\tilde{\chi}''_{\rm rd} - \tilde{\chi}''}{\tilde{\chi}''_{\rm rd}} \sim \frac{1}{\kappa\langle x^3\rangle}, \tag{62}$$

thus, the relative error of calculations by the rigid dipole model does not exceed 10% if $\kappa\langle x^3\rangle \gtrsim 10$.

From the results obtained, it is evident that the dc field can significantly affect the dynamic magnetic susceptibility of nanoparticles suspended in a fluid. For an ensemble satisfying condition Eq. (61), the biasing causes mainly quantitative modifications: reduction of the height of both (low- and high-frequencies) absorption maxima and noticeable shift of the low-frequency one to the right—to higher frequencies. The effect depends on the anisotropy of particles: the weaker it is, the more significant changes in the frequency range $\omega\tau_M \gtrsim \zeta_0$. This fact is confirmed yet again by Figs. 13(a) and 13(b), where the Cole-Cole diagrams are shown for suspensions with the same disperse composition ($\langle x\rangle = 1.4$, $\delta = 0.2$), but different values of the anisotropy parameter: $\kappa = 20$, 5 and 2, respectively.

If particle-size distribution obeys the opposite inequality, then the dc field can lead to qualitative changes, namely, to the appearance or disappearance of absorption peaks and, associated with them, sharp decreases in the real component of the susceptibility. A vivid illustration is the bias-induced emergence of the additional low-frequency maximum in the $\tilde{\chi}''(\omega)$ spectrum, provided an ensemble meets the condition Eq. (60), see dashed line in Fig. 13(c) as an example. Note this effect does not imply a very narrow distribution of particle diameters and/or their ultra small values. For example, for particles with the anisotropy constant $K \sim 10^5$ erg/cm^3 and saturation magnetization $M_s \approx 400$ emu/ cm^3 the specified condition is fulfilled by an ensemble with the average magnetic diameter $\langle d\rangle \approx 8$ nm and the relative distribution width $\delta = 0.3$.

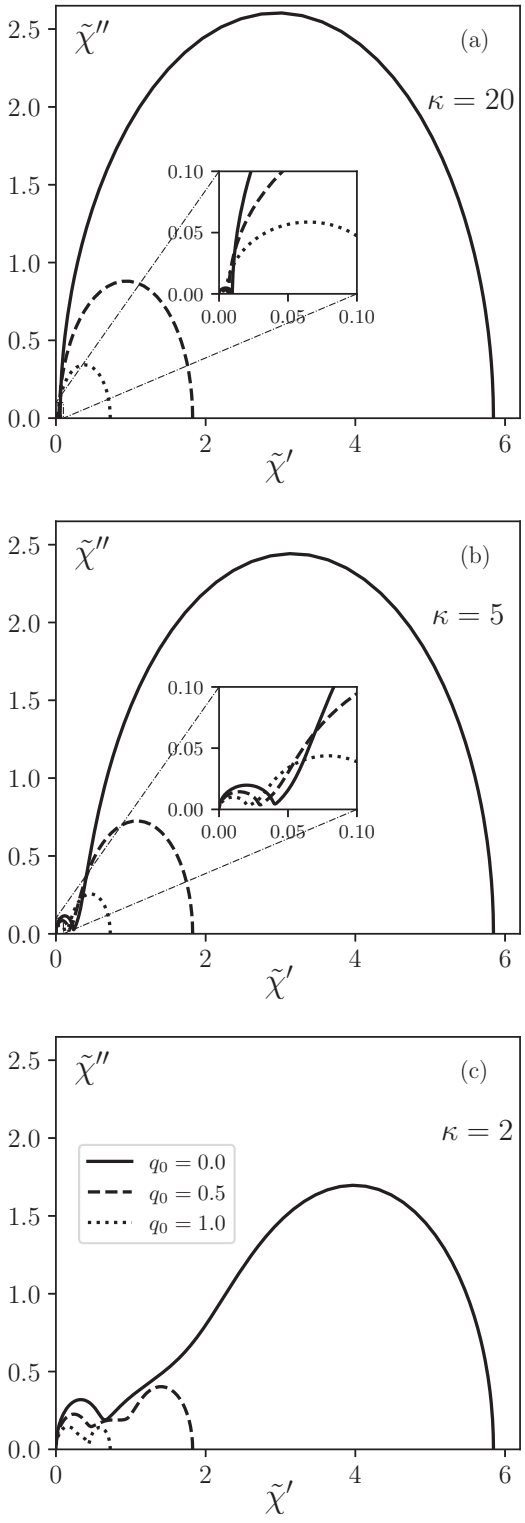

FIG. 13. Cole-Cole diagrams of polydisperse ensembles of nanoparticles, suspended in a fluid (average magnetic diameter $\langle x \rangle = 1.4$, relative standard deviation $\delta = 0.25$) at anisotropy parameter $\kappa = 20$ (a), 5 (b), and 2 (c); solid lines: bias field $q_0 = 0$, dashes: $q_0 = 0.5$, dots: $q_0 = 1$; viscosity parameter $\zeta_0 = 10^{-3}$, surfactant thickness $x_s = 0.5$.

Interparticle dipole-dipole interactions are not considered in the present paper. A consistent description of the interaction effects is one of the key problem in the theory of the dynamic magnetic response of ferrofluids. It is very hard (in real systems, a number of particles is huge and their volume concentration is typically not small) and its detailed discussion goes beyond the scope of this paper. However, it is worthy to mention that in magnetic suspensions the specified interactions can mainly lead to (a) aggregation of particles, that is, effective growth of their size, (b) modification of a particle anisotropy constant, and (c) change of the magnetic field acting on each particle. These assertion follows from general properties of the dipole potential and laborious numerical calculations, performed by different approaches such as a mean-field theory (see, e.g., Refs. [25,26]), Brownian simulations (see, e.g., Refs. [27,28]), Langevin dynamics (see, for example, Refs. [29,30]), and the so-called diffusion-jump model [31,32]. Besides, to explain experimental results, it is sometimes believed that an external dc field stimulates the growth of chains of particles in a ferrofluid (see, e.g., Ref. [33]).

Evidently, none of the specified interaction effects can lead to a magnetic response of an ensemble in the frequency range $\omega\tau_M \gtrsim 10^{-1}$ if there is no signal from any individual particle. Also, if particles are superparamagnetic, then neither their enlargement nor a finite change of the anisotropy constant (its possible correction due to dipole-dipole interaction hardly exceeds $\sim M_s^2$) nor a change in the acting field by a value of $\sim M_s$ (expected order of an effective field modeling the interparticle interactions) causes zeroing out of the real part of the dynamic susceptibility at frequencies $\omega\tau_M \gtrsim \zeta_0$ or imaginary part at $\omega\tau_M \gtrsim 10^{-1}$. Note also that even in the case when the local magnetic field in a suspension differs from the applied one due to the dipole-dipole interactions the effect of the bias field will be the stronger, the weaker anisotropy of particles.

Taking this into account, one can make a qualitative interpretation of experimental data from Ref. [34], where the Cole-Cole diagrams for two magnetic fluids (not diluted)—based on cobalt ferrite particles (with volume concentration

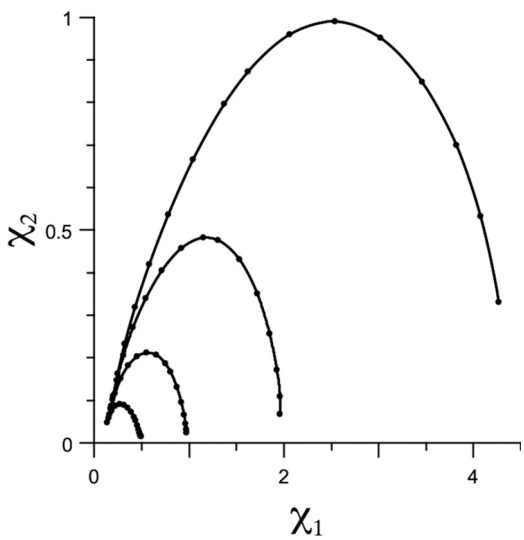

FIG. 14. Experimentally found Cole-Cole diagrams for the magnetic fluid based on cobalt ferrite particles at different values of the bias field: 0, 3, 6, 12 kA/m (the field increases from up to down and from right to left); temperature $t = 25\,^{\circ}$C. Figure is taken from Ref. [34] with the consent of A.V. Lebedev.

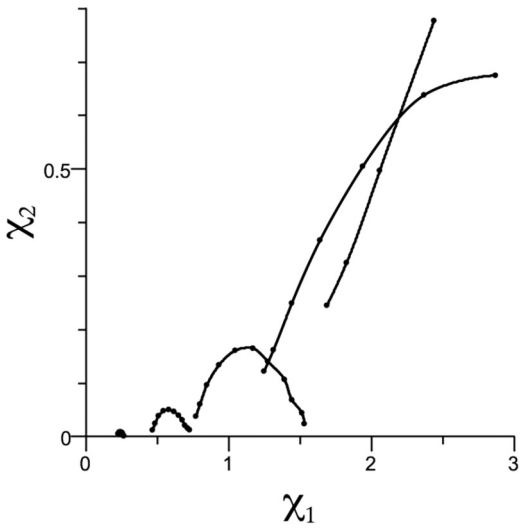

FIG. 15. Experimentally found Cole-Cole diagrams for the magnetic fluid based on magnetite particles at different values of the bias field: 0, 2, 5, 10, 24 kA/m (the field increases from up to down and from right to left); temperature $t = 25\,^{\circ}$C. Figure is taken from Ref. [34] with the consent of A.V. Lebedev.

1.3×10^{17} cm $^{-3}$) and based on magnetite particles (with concentration 3.7×10^{16} cm^{-3})—are measured in dc field. With kind consent of A.V. Lebedev, the author of these experiments, the obtained results are reproduced in Figs. 14 and 15, respectively. In the experiments, frequency of the probing field has not exceeded 200 kHz, so details of the high-frequency response are not completely revealed. However, one can see that for the both suspensions the Cole-Cole diagrams tend not to cross the origin of coordinates—in accordance with the theoretical predictions for superparamagnetic systems. Also, for the sample with strongly anisotropic cobalt ferrite particles the bias field almost does not affect the extrapolation point at which the diagrams intersect the abscissa axis. In opposite, its effect on the high-frequency response (sections of the diagrams to the left of the maximum point) of magnetite particles with relatively small anisotropy constant is significant. This is in a qualitative agreement with results of the above analysis (compare Figs. 14 and 15 with Fig. 13).

VI. CONCLUSION

A kinetic theory of the linear magnetic response of single-domain uniaxial particles suspended in a fluid is presented. On that basis, possible types of frequency dependence of the longitudinal dynamic susceptibility of such particles are outlined. It is shown that the ratio of anisotropy energy to thermal energy should not be considered as the exclusive measure of superparamagnetism: for the same value of the specified quantity, the signal from particles with strong (e.g., cobalt ferrite) and weak or moderate (e.g., magnetite) anisotropy is qualitatively different if a bias field is applied.

The proposed description is extended to polydisperse suspensions of noninteracting nanoparticles with a finite strength of the magnetic anisotropy. It is shown that generally superparamagnetic effects in the magnetic response of such systems are not vanished away and completely disappear only in the case of quasistatic remagnetization. The internal diffusion of the magnetic moment of particles leads at least to quantitative changes of the dynamic magnetic susceptibility. The estimates of these corrections in different frequency bands are performed for suspensions of strongly anisotropic particles. However, for polydisperse ensembles of particles with weak or moderate anisotropy, the internal degrees of freedom of the magnetic moment can cause a splitting of the absorption spectrum. In principle, for ensembles of particles with strong anisotropy, this effect is also possible but the particle-size distribution must satisfy quite serious restrictions. It is confirmed that at any finite value of the particle anisotropy constant and for any type of the polydispersity, the dynamic magnetic susceptibility of a ferrofluid at high ($100\,\text{kHz} \lesssim f \lesssim 10\,\text{GHz}$) frequencies is expected to be nonzero even if gyration of the magnetic moment is not taken into account.

The significant effect of the bias field on the magnetic response of the system is shown. First, it can induce an additional maximum in the frequency sweep of the imaginary part of the dynamic magnetic susceptibility and this effect does not at all require that all particles have the same size. Second, it allows us to evaluate how important it is to consider superparamagnetism of particles, namely, without a biasing, the frequency spectra of the dynamic magnetic susceptibility for ensembles of strongly and weakly anisotropic particles may be of the same type due to a polydispersity. However, the effect of the dc field will be stronger for particles with smaller anisotropy and thereby have more pronounced superparamagnetic properties.

The developed computational scheme does not include the interparticle dipole-dipole interactions and, strictly speaking, it is usable for dilute ferrofluids only. However, the estimates allow us to infer that for the interacting particles as well as for the noninteracting ones, the high-frequency response should be significant and the effect of the bias field should be more noticeable, the stronger the thermal fluctuations of the magnetic moment inside particles. This conclusion qualitatively agrees with experimental data.

ACKNOWLEDGMENTS

The work was supported by Russian Science Foundation under Grant No. 22-22-00288. The author thanks A. V. Lebedev and M. A. Koskov for fruitful discussions of the problem.

[1] L. Néel, Ann Géophys. **5**, 99 (1949).
[2] C. P. Bean, J. Appl. Phys. **26**, 1381 (1955).
[3] A. Rivera-Rodriguez and C. M. Rinaldi-Ramos, Annu. Rev. Chem. Biomol. Eng. **12**, 163 (2021).

[4] A. Baki, F. Wiekhorst, and R. Bleul, Bioengineering **8**, 134 (2021).
[5] H. Gavilán, K. Simeonidis, E. Myrovali, E. Mazario, O. Chybykalo-Fesenko, R. Chantrell, L. Balcells, M. Angelakeris, M. P. Morales, and D. Serantes, Nanoscale **13**, 15631 (2021).
[6] C. Turrina, D. Milani, A. Klassen, D. M. Rojas-González, J. Cookman, M. Opel, B. Sartori, P. Mela, S. Berensmeier, and S. P. Schwaminger, Int. J. Mol. Sci. **23**, 14743 (2022).
[7] W. T. Coffey and Yu.. P. Kalmykov, J. Appl. Phys. **112**, 121301 (2012).
[8] W. T. Coffey, Yu. P. Kalmykov, and S. V. Titov, *Thermal Fluctuations and Relaxation Processes in Nanomagnets* (World Scientific, Singapore, 2020).
[9] V. I. Stepanov and M. I. Shliomis, Bull. Acad. Sci. USSR, Phys. Ser. **55**, 1042 (1991).
[10] Yu. L. Raikher and V. I. Stepanov, Adv. Chem. Phys. **129**, 419 (2004).
[11] R. Taukulis and A. Cēbers, Phys. Rev. E **86**, 061405 (2012).
[12] J. Weizenecker, Phys. Med. Biol. **63**, 035004 (2018).
[13] S. V. Titov, W. T. Coffey, Yu. P. Kalmykov, M. Zarifakis, and A. S. Titov, Phys. Rev. E **103**, 052128 (2021).
[14] P. Ilg and M. Kröger, Phys. Rev. B **106**, 134433 (2022).
[15] I. S. Poperechny, Phys. Rev. B **107**, 064416 (2023).
[16] I. S. Poperechny, J. Mol. Liq. **299**, 112109 (2020).
[17] M. A. Martsenyuk, Y. L. Raikher, and M. I. Shliomis, Zh. Eksp. Teor. Fiz. **65**, 834 (1973).
[18] D. A. Krueger, J. Appl. Phys. **50**, 8169 (1979).
[19] Y. L. Raikher and V. I. Stepanov, Phys. Rev. B **66**, 214406 (2002).
[20] Yu. L. Raikher and V. I. Stepanov, J. Magn. Magn. Mater. **368**, 421 (2014).
[21] Yu. L. Raikher and V. I. Stepanov, Phys. Rev. B **50**, 6250 (1994).
[22] J. Dieckhoff, D. Eberbeck, M. Schilling, and F. Ludwig, J. Appl. Phys. **119**, 043903 (2016).
[23] A. V. Lebedev, J. Magn. Magn. Mater. **374**, 120 (2015).
[24] I. S. Poperechny, Yu. L. Raikher, and V. I. Stepanov, J. Magn. Magn. Mater. **424**, 185 (2017).
[25] A. O. Ivanov, V. S. Zverev, and S. S. Kantorovich, Soft Matter **12**, 3507 (2016).
[26] A. O. Ivanov and P. J. Camp, Phys. Rev. E **102**, 032610 (2020).
[27] J. O. Sindt, P. J. Camp, S. S. Kantorovich, E. A. Elfimova, and A. O. Ivanov, Phys. Rev. E **93**, 063117 (2016).
[28] P. J. Camp, A. O. Ivanov, and J. O. Sindt, Phys. Rev. E **103**, 062611 (2021).
[29] A. F. Pshenichnikov and A. A. Kuznetsov, Phys. Rev. E **92**, 042303 (2015).
[30] P. Ilg, Phys. Rev. B **95**, 214427 (2017).
[31] P. Ilg and M. Kröger, Phys. Chem. Chem. Phys. **22**, 22244 (2020).
[32] P. Ilg and M. Kröger, Sci. Rep. **13**, 16523 (2023).
[33] A. Pshenichnikov, A. Lebedev, and A. O. Ivanov, Nanomaterials **9**, 1711 (2019).
[34] A. V. Lebedev, Bulletin of Perm University, Physics, no. 4, 14 (2021).